ISA Transactions xxx (xxxx) xxx

Contents lists available at ScienceDirect

ISA Transactions

journal homepage: www.elsevier.com/locate/isatrans

Research article

Event-triggered robust distributed output feedback model predictive control for nonlinear MASs against false data injection attacks

Zhengcai Li [a], Huiling Xu [a,*], Zhiping Lin [b], Lewei Dong [a], Yuqing Chen [a]

[a] School of Mathematics and Statistics, Nanjing University of Science and Technology, Nanjing, 210094, China
[b] School of Electrical and Electronic Engineering, Nanyang Technological University, Singapore, 639798, Singapore

ARTICLE INFO

Article history:
Received 8 February 2023
Received in revised form 18 June 2023
Accepted 30 June 2023
Available online xxxx

Keywords:
Distributed output feedback model predictive control
False data injection attacks
Robust multivariate observer
Event-triggered mechanism

ABSTRACT

In this paper, an event-triggered distributed output feedback model predictive control scheme for the nonlinear disturbed multiagent systems with sensor–controller channel false data injection attacks is proposed. To provide valid system states to the controller in the event of cyber attacks, a robust multivariate observer is designed to realize the estimation and separation of uncompromised system states, false data injection attacks, and measurement disturbances, simultaneously. Based on these reconstructed signals and a newly-designed linear robustness constraint, the distributed predictive controller is established to achieve smooth cooperative stabilization among agents. Meanwhile, an event-triggered mechanism is applied to save computing resources, and it restricts the error of predictive states and estimated states to guarantee the feasibility of the optimization control problem. Theoretical analyses on robustness and security for the nonlinear multiagent systems under event-triggered distributed output feedback model predictive control are presented. Finally, a simulation on two pairs of one-link flexible joint manipulator systems verifies the theoretical results.

1. Introduction

Cooperation and consensus in multiagent systems (MASs) have been richly researched with plenty of technological advancements in computing and communication for the last decades [1–3]. Their applications spread across formation control, flocking, and vehicle cooperative control [4–6]. Among these varieties of research fields, the cooperation of nonlinear MASs has been developed deeply [7–9]. Prior research on MASs with general linear and Lipschitz nonlinear dynamics can be found in [10–12]. As networked communication plays an essential role in MASs, the intensifying cyber adversarial environment brought more constraints and challenges to current research [13,14].

Distributed model predictive control (DMPC), which explicitly considers multiple constraints while providing optimal control performance, has become a popular approach to the security issues of MASs [15,16]. From the perspective of corruption effects, cyber attacks can be divided into deception attacks (false data injection (FDI) attacks and replay attacks) and disruption attacks (denial-of-service (DoS) attacks and jamming attacks) [17–19]. Meanwhile, The vulnerability of communication channels intra-agent (sensor–controller (S–C) and controller–actuator (C–A)) becomes a potential target point for adversaries gradually, and few studies have addressed this issue under the DMPC scheme [20–23]. In [20,21], distributed constraint regulation and cooperative stabilization problems of MAS have been addressed in the presence of dual-channel DoS attacks. S–C replay attacks in linear MAS have been dealt with identification and isolation mechanism in [22], respectively. In [23], a new economic DMPC strategy with an intrusion detector is proposed for linearly coupled MAS in the presence of S–C FDI attacks. Observing from the above literature, the S–C FDI attacks corrupt the availability of the state in the predictive control scheme, and the DMPC strategies for nonlinear MAS have not been explored.

Different from the general DMPC, distributed output feedback MPC (DOFMPC) takes the main role in systems where the states are not measurable, which is the same scenario of S–C FDI attacks on MASs. In [24], the leader–follower consensus of linear MAS with a directed graph has been investigated. The static robust OFMPC and dynamic DOFMPC for state-coupled linear MAS can be found in [25,26], respectively. In [27], an interval observer-based robust OFMPC for linear MAS with state and control constraints. Different from the above research that mainly considers the satisfaction of constraints in time-invariant systems, DOFMPC for unconstrained time-varying systems has also received some attention [28,29]. In [28], an off-line OFMPC approach has been studied for constrained linear parameter varying systems subject to bounded disturbances. In [29], it addressed the OFMPC of

* Corresponding author.
E-mail addresses: lizhengcai0224@njust.edu.cn (Z. Li), xuhuiling@njust.edu.cn (H. Xu), EZPLin@ntu.edu.sg (Z. Lin), donglewei@126.com (L. Dong), chenyuqing@njust.edu.cn (Y. Chen).

https://doi.org/10.1016/j.isatra.2023.06.039
0019-0578/

the constrained polytopic uncertain system in the presence of bounded state and output disturbances. These studies motivate us to investigate the potential of applying the DOFMPC scheme to attack scenarios.

Besides cyber attacks, disturbances are another factor that cannot be disregarded in actual systems. Under a predictive control scheme, disturbances brought differences between the actual and predicted systems, and this error can be confined by employing a trigger mechanism. Compare to the self-triggered mechanism applied in the consensus problem of a nonlinear discrete-time MAS [30,31], event-triggered mechanisms are more widely used in MPC control problems in the security field [16,19,32]. From the above observations, the robustness and security problems of MAS are still not addressed through the DOFMPC strategies. It is of great interest to find an effective DOFMPC solution for the attacked disturbed nonlinear MAS.

To tackle the robustness and security problem for the nonlinear MASs, this paper proposed an event-triggered DOFMPC scheme for nonlinear MASs to defend against S–C FDI attacks and disturbances. Structurally, a decentralized robust multivariate observer (RMO) is constructed to eliminate attack effects locally, and a distributed predictive controller using estimated states and containing newly linear robustness constraints is designed for nonlinear MAS to achieve robust cooperative stabilization. Furthermore, an event-triggered mechanism is embedded in the controller to sustain feasibility and save computing resources.

The main contributions of this paper are summarized in the following:

1. A robust secure DOFMPC scheme against S–C FDI attacks and disturbances is proposed for nonlinear MASs for the first time. This secure solution consists of a newly-designed decentralized RMO and a distributed output feedback model predictive controller with an event-triggered mechanism, which separates the uncompromised states from FDI attacks and drives all agents into cooperation.
2. A novel linear robustness constraint is built into the optimization control problem (OCP) of the predictive controller. Compare to the existing works [8,9,12], it smooths out the shrinkage process of the predictive states, which prevents the predictive control sequence from frequent oscillations. Moreover, an event-triggered mechanism that dynamically adjusts the renewal of the prediction sequence is proposed to effectively save computational resources.
3. Theoretical analyses for the event-triggered DOFMPC scheme, including the recursive feasibility of distributed OCP and the cooperation among agents, are established. It proves that the proposed scheme deals with the impacts of S–C FDI attacks and ensures the robust performance of the nonlinear MAS effectively.

The rest of this paper is organized as follows. In Section 2, a system description and some general assumptions are given. In Section 3, an attack separable RMO and a robust DOFMPC method are proposed. The main results involving the recursive feasibility and the cooperation of MAS are developed in Section 4. In Section 5, a simulation example is given to illustrate the obtained results, and the conclusion of this paper is given in Section 6.

Notation. $\mathbb{N}$, $\mathbb{R}^n$ and $\mathbb{R}^{p\times n}$ represent the set of non-negative integers, n-dimensional Euclidean space, and the set of $p \times n$ real matrices, respectively. I_n and $O_{n\times p}$ denote the n-dimensional identity matrix and $n \times p$ dimensional zero matrix. The notation $\mathbb{N}_{[1,N-1]}$ indicates the sets $\{r \in \mathbb{N} | 1 \le r \le N-1\}$. The smallest and largest eigenvalues of a matrix are denoted by $\lambda_{\min}(\cdot)$ and $\lambda_{\max}(\cdot)$, respectively. For $P \in \mathbb{R}^{n\times n}$, let $\rho(P)$ denote the spectral radius of P, the notation $P > 0$ denotes symmetric positive definiteness, P^T denotes transpose of P, and $\|P\| = \sqrt{\lambda_{\max}(P^TP)}$. For a symmetric $n \times n$ positive definite matrix W and $h \in \mathbb{R}^n$, $\|h\|^2 = h^Th$ and $\|h\|_W^2 = h^TWh$. The predicted time sequence at t_h is denoted as $\{s|t_h\}$, $s \in \mathbb{N}_{[t_h.t_h+N_p]}$, and N_p is the prediction horizon of controller. In the expression for the internal structure of a matrix, $\star$ represents the transpose matrix in the symmetric position. $\Omega(\epsilon)$ denotes the neighborhood of the origin with ϵ as its radius.

2. Preliminaries and problem formulation

Consider the discrete-time heterogeneous nonlinear MAS consisting of M agents, and the dynamics of each agent i, $i \in \mathbb{N}_{[1,M]}$, are given as

$$\begin{cases} x_i(k+1) = A_ix_i(k) + B_iu_i(k) + G_ig_i\big(x_i(k)\big) + D_{ix}\omega_{ix}(k), & \text{(a)} \\ y_i(k) = C_ix_i(k) + D_{iy}\omega_{iy}(k) + S_ia_{iy}(k), & \text{(b)} \end{cases} \tag{1}$$

where $x_i(k) \in \mathbb{R}^{n_x}$, $u_i(k) \in \mathcal{U}_i$, $y_i(k) \in \mathbb{R}^{n_y}$, $\omega_{ix}(k) \in \mathbb{R}^{n_{\omega x}}$, $\omega_{iy}(k) \in \mathbb{R}^{n_{\omega y}}$ and $a_{iy}(k) \in \mathbb{R}^{n_a}$ are the system states, control inputs, measurable outputs, system disturbances, measurement disturbances, and S–C FDI attacks respectively. $\mathcal{U}_i \subseteq \mathbb{R}^{n_u}$ is the control constraint of each agent. A_i, B_i, C_i, G_i, D_{ix}, D_{iy}, S_i are constant real matrices with appropriate dimensions. $g_i\big(x_i(k)\big) \in \mathbb{R}^{n_g}$ is the nonlinear function representing the local nonlinear dynamics of the agent, which is Lipschitz with respect to $x_i(k)$, i.e.,

$$\|g_i\big(x_a(k)\big) - g_i\big(x_b(k)\big)\| \le c\|x_a(k) - x_b(k)\|. \tag{2}$$

To model the communication topology among agents, an undirected graph $\mathcal{G} = (\mathcal{V}, \mathcal{E})$ is introduced, where $\mathcal{V} = \mathbb{N}_{[1,M]}$ represents the collection of vertices and $\mathcal{E} \subseteq \big\{(i,j) \in \mathcal{V}\times\mathcal{V} | i \ne j\big\}$ is the edge set indicating the interconnection among agents. The neighboring vertex set of agent i is denoted as $\mathcal{N}_i = \big\{j \in \mathcal{V} | (i,j) \in \mathcal{E}\big\}$.

Some general assumptions are given as follows.

Assumption 1. (A_i, B_i) is stabilizable, and $\mathcal{G}$ is connected.

Assumption 2. The system disturbance $\omega_{ix}(k)$ is bounded as follows:

$$\sum_{k=0}^{\infty} \omega_{ix}^T(k)\omega_{ix}(k) = \varpi_i. \tag{3}$$

Assumption 3. The matrix $[D_{iy}\ S_i]$ is of full column rank, and the S–C FDI attacks and measurement disturbances are distinguishable [33].

Remark 1. In Assumption 2, energy-bounded system disturbance ω_{ix} is commonly adopted in robust H_∞ MPC [19,34]. The observation of system states, cyber-attacks, and measurement disturbances can be attained with an H_∞ performance on this basis. Similar to [33], the full column assumption of the matrix $[D_{iy}\ S_i]$ in Assumption 3 implies that FDI attacks and measurement disturbances are linearly independent, which allows them to be separated.

In this paper, we mainly focus on the robust secure control problem of nonlinear MAS with S–C FDI attacks, measurement disturbances, and system disturbances. For MAS (1)(a), only compromised outputs y_i are accessible for remote controllers, which implies that an observer is required for the MPC to estimate and deliver uncompromised states. Meanwhile, the interconnection between agents, along with system disturbance and observation error may lead to the failure of the predictive controller,

which could be confined by a triggering mechanism. Confronting those problems, the main objective of this paper is to design an observer-based robust secure MPC scheme with an event-triggered mechanism for the nonlinear MAS (1)(a), such that the agents are cooperatively stabilized toward the origin.

3. Event-triggered distributed output feedback model predictive control

In this section, a robust multivariate observer (RMO), an event-triggered mechanism, and a predictive controller of the proposed robust secure DMPC scheme are presented. Structurally, before the predictive controller is misguided by the compromised output, an RMO is introduced to estimate uncompromised system states and use it as controller input. After the predictive controller generates the effective predicted control sequence, an event-triggered mechanism is designed to restrain the state error between the actual system and the predictive system.

3.1. Attack separable robust multivariate observer

From the perspective of predictive controllers, it is important to obtain uncompromised system states to generate effective control. Therefore, uncompromised system states should be separated from FDI attacks. To achieve this goal, an augmented system and decentralized RMO are proposed in this subsection.

An augmented system is established to facilitate the decentralized RMO design.

First denote $z_i(k) = \left[x_i^T(k),\ \omega_{iy}^T(k),\ a_{iy}^T(k)\right]^T$, and the dynamics of the system can be obtained from (1) as

$$\begin{cases} H_{i0}z_i(k+1) = A_{i0}z_i(k) + B_{i0}u_i(k) + G_{i0}g_i\big(x_i(k)\big) \\ \quad +D_{i0}\omega_{ix}(k) + Z_{i0}y_i(k), & \text{(a)} \\ y_i(k) = C_{i0}z_i(k), & \text{(b)} \end{cases} \tag{4}$$

where

$$H_{i0} = \begin{bmatrix} I_{n_x} & O_{n_x\times(n_{\omega y}+n_a)} \\ O_{n_y\times n_x} & O_{n_y\times(n_{\omega y}+n_a)} \end{bmatrix},$$

$$A_{i0} = \begin{bmatrix} A_i & O_{n_x\times n_{\omega y}} & O_{n_x\times n_a} \\ -C_i & -D_{iy} & -S_i \end{bmatrix},\ B_{i0} = \begin{bmatrix} B_i \\ O_{n_y\times n_u} \end{bmatrix},$$

$$G_{i0} = \begin{bmatrix} G_i \\ O_{n_y\times n_g} \end{bmatrix},$$

$$C_{i0} = \begin{bmatrix} C_i & D_{iy} & S_i \end{bmatrix},\ Z_{i0} = \begin{bmatrix} O_{n_x\times n_y} \\ I_{n_y} \end{bmatrix},\ D_{i0} = \begin{bmatrix} D_{ix} \\ O_{n_y\times n_{\omega x}} \end{bmatrix}.$$

Select $N_{i0} = \begin{bmatrix} O_{n_x\times n_y} \\ I_{n_y} \end{bmatrix}$ and add $N_{i0}C_{i0}z_i(k+1)$ to both sides of the first equation in (4)(a), then one has

$$\begin{aligned} H_{i1}z_i(k+1) = {} & A_{i0}z_i(k) + B_{i0}u_i(k) + G_{i0}g_i\big(x_i(k)\big) \\ & + D_{i0}\omega_{ix}(k) + Z_{i0}y_i(k) + N_{i0}y_i(k+1), \end{aligned} \tag{5}$$

where $H_{i1} = H_{i0} + N_{i0}C_{i0}$. According to Assumption 3, $H_{i1} = \begin{bmatrix} I_{n_x} & O & O \\ C_i & D_{iy} & S_i \end{bmatrix}$ is a full column rank matrix as matrix $\begin{bmatrix} D_{iy} & S_i \end{bmatrix}$ is of full column rank. Let $\bar{H}_{i1}$ be the left inverse of H_{i1}, i.e., $\bar{H}_{i1}H_{i1} = I_{(n_x+n_{\omega y}+n_a)}$, therefore (4)(a) can be rewritten as

$$\begin{aligned} z_i(k+1) = {} & A_{i1}z_i(k) + B_{i1}u_i(k) + G_{i1}g_i\big(x_i(k)\big) + D_{i1}\omega_{ix}(k) \\ & + Z_{i1}y_i(k) + \bar{H}_{i1}N_{i0}y_i(k+1), \end{aligned} \tag{6}$$

where $A_{i1} = \bar{H}_{i1}A_{i0}$, $B_{i1} = \bar{H}_{i1}B_{i0}$, $G_{i1} = \bar{H}_{i1}G_{i0}$, $D_{i1} = \bar{H}_{i1}G_{i0}$, $Z_{i1} = \bar{H}_{i1}Z_{i0}$. Denote $\xi_i(k+1) = z_i(k+1) - \bar{H}_{i1}N_{i0}y_i(k+1)$, and the augmented system dynamics of agent i under FDI attacks are eventually rewritten as

$$\xi_i(k+1) = A_{i1}\xi_i(k) + B_{i1}u_i(k) + G_{i1}g_i\big(x_i(k)\big) + D_{i1}\omega_{ix}(k) + Z_{i2}y_i(k), \tag{7}$$

where $Z_{i2} = Z_{i1} + A_{i1}\bar{H}_{i1}N_{i0}$.

In the following, an RMO is introduced to estimate uncompromised states $x_i(k)$, measurement disturbances $\omega_{iy}(k)$ and FDI attacks $a_{iy}(k)$, each of which can be separated from the estimated intermediate variables $z_i(k)$.

$$\begin{cases} \hat{\xi}_i(k+1) = A_{i1}\hat{\xi}_i(k) + B_{i1}u_i(k) + G_{i1}g_i\big(\hat{x}_i(k)\big) \\ \quad +Z_{i2}y_i(k) + L_i\big(y_i(k) - \hat{y}_i(k)\big), & \text{(a)} \\ \hat{z}_i(k) = \hat{\xi}_i(k) + \bar{H}_{i1}N_{i0}y_i(k), & \text{(b)} \\ \hat{y}_i(k) = C_{i0}\hat{z}_i(k), & \text{(c)} \\ \hat{x}_i(k) = \mathcal{I}_x\hat{z}_i(k), & \text{(d)} \\ \hat{\omega}_{iy}(k) = \mathcal{I}_\omega\hat{z}_i(k), & \text{(e)} \\ \hat{a}_{iy}(k) = \mathcal{I}_a\hat{z}_i(k), & \text{(f)} \end{cases} \tag{8}$$

where $\hat{\xi}_i(k)$, $\hat{y}_i(k)$, $\hat{z}_i(k)$, $\hat{x}_i(k)$, $\hat{\omega}_{iy}(k)$, $\hat{a}_{iy}(k)$ are observer states, estimations of outputs, augmented states, uncompromised states, measurement disturbances, and FDI attacks, respectively.

In the light of observer (8)(b) and definition of intermediate variables $z_i(k)$, the separation matrices in (8)(d)–(8)(f) are given as $\mathcal{I}_x = \begin{bmatrix} I_{n_x} & O_{n_x\times n_\omega} & O_{n_x\times n_a} \end{bmatrix}$, $\mathcal{I}_\omega = \begin{bmatrix} O_{n_\omega\times n_x} & I_{n_\omega} & O_{n_\omega\times n_a} \end{bmatrix}$, $\mathcal{I}_a = \begin{bmatrix} O_{n_a\times n_x} & O_{n_a\times n_\omega} & I_{n_a} \end{bmatrix}$.

Remark 2. The RMO is derived from a Luenberger-like observer and serves for the augmented system (7). Inspired by [35,36], additive FDI attacks can be separated from uncompromised states using multivariate step-by-step conversion. With the help of the designed RMO, the uncompromised system states can be estimated and delivered to the remote controller to guarantee an effective control performance.

Define estimation errors as $e_{\xi_i}(k) \triangleq \xi_i(k) - \hat{\xi}_i(k)$, $e_{z_i}(k) \triangleq z_i(k) - \hat{z}_i(k)$, $e_{x_i}(k) \triangleq x_i(k) - \hat{x}_i(k)$, and $e_{y_i}(k) \triangleq y_i(k) - \hat{y}_i(k)$. From the definitions of estimation errors and RMO, one has $e_{\xi_i}(k) = e_{z_i}(k)$. Combining (6) and (8)(a)–(8)(c), the error dynamics can be described as follows

$$\begin{aligned} e_{z_i}(k+1) &= e_{\xi_i}(k+1) \\ &= A_{Li}e_{\xi_i}(k) + G_{i1}e_{g_i}(k) + D_{i1}\omega_{ix}(k) \\ &= A_{Li}e_{z_i}(k) + G_{i1}e_{g_i}(k) + D_{i1}\omega_{ix}(k), \end{aligned} \tag{9}$$

where $e_{g_i}(k) \triangleq g_i(x_i(k)) - g_i(\hat{x}_i(k))$, $A_{Li} = A_{i1} - L_iC_{i0}$.

Lemma 1. *For the given Lipschitz constant c, the augmented error system (9) is asymptotically stable with H_∞ performance level γ, if there exist positive definite matrix F_i, matrix $\mathcal{F}_i$ and positive constant μ_i, such that the following inequality condition holds:*

$$\begin{bmatrix} -F_i + \mu_i c^2\mathcal{I}_x^T\mathcal{I}_x & O & O & A_{i1}^TF_i - C_{i0}^T\mathcal{F}_i^T \\ \star & -\mu_iI_{n_g} & O & G_{i1}^TF_i \\ \star & \star & -\gamma^2I_{n_{\omega x}} & D_{i1}^TF_i \\ \star & \star & \star & -F_i \end{bmatrix} < 0 \tag{10}$$

and the observation gain matrix is chosen as $L_i = F_i^{-1}\mathcal{F}_i$.

Proof. For the error dynamic system (9), the Lyapunov function is chosen as

$$\mathcal{V}_e(k) = e_{z_i}^T(k)F_ie_{z_i}(k) \tag{11}$$

where $F_i > 0$. Utilizing the trajectory of error system (9) to calculate the difference of $\mathcal{V}_e(k)$, it can be obtained that

$$\begin{aligned}\Delta\mathcal{V}_e(k) =&\mathcal{V}_e(k+1)-\mathcal{V}_e(k)\\ =&e_{z_i}^T(k+1)Fe_{z_i}(k+1)-e_{z_i}^T(k)Fe_{z_i}(k)\\ =&\|A_{Li}e_{z_i}(k)+G_{i1}e_{g_i}(k)+D_{i1}\omega_{ix}(k)\|_{F_i}^2-\|e_{z_i}\|_{F_i}^2\\ =&\|e_{z_i}\|_{A_{Li}^TF_iA_{Li}-F_i}^2+2e_{g_i}^T(k)G_{i1}^TF_iA_{Li}e_{z_i}(k)+\|G_{i1}e_{g_i}(k)\|_{F_i}^2\\ &+2e_{g_i}^T(k)G_{i1}^TF_iD_{i1}\omega_{ix}(k)+2\omega_{ix}^T(k)D_{i1}^TF_iA_{Li}e_{z_i}(k)\\ &+\|D_{i1}\omega_{ix}(k)\|_{F_i}^2.\end{aligned}\tag{12}$$

(i) In the case of $\omega_{ix}(k)=0$, one has

$$\Delta\mathcal{V}_e(k)=\|e_{z_i}\|_{A_{Li}^TF_iA_{Li}-F_i}^2+\|G_{i1}e_{g_i}(k)\|_{F_i}^2+2e_{g_i}^T(k)G_{i1}^TF_iA_{Li}e_{z_i}(k).\tag{13}$$

Based on Lipschitz condition and (8)(d), we have

$$e_{g_i}^T(k)e_{g_i}(k)\le c^2e_{x_i}^T(k)e_{x_i}(k)\le c^2e_{z_i}^T(k)\mathcal{I}_x^T\mathcal{I}_xe_{z_i}(k).\tag{14}$$

Consequently, one has

$$\begin{aligned}\Delta\mathcal{V}_e(k)\le&\|e_{z_i}\|_{A_{Li}^TF_iA_{Li}-F_i}^2+\|G_{i1}e_{g_i}(k)\|_{F_i}^2+2e_{g_i}^T(k)G_{i1}^TF_iA_{Li}e_{z_i}(k)\\ &-\mu_ie_{g_i}^T(k)e_{g_i}(k)+\mu_ic^2e_{z_i}^T(k)\mathcal{I}_x^T\mathcal{I}_xe_{z_i}(k),\end{aligned}\tag{15}$$

where μ_i is a positive constant. We can also represent the above inequality as

$$\Delta\mathcal{V}_e(k)\le\mathcal{E}^T(k)\Theta\mathcal{E}(k),\tag{16}$$

where $\mathcal{E}(k)=\left[e_{z_i}^T(k)\ e_{g_i}^T(k)\right]^T$, and

$$\Theta=\begin{bmatrix}A_{Li}^TF_iA_{Li}-F_i+\mu_ic^2\mathcal{I}_x^T\mathcal{I}_x & A_{Li}^TF_iG_{i1}\\ \star & G_{i1}^TF_iG_{i1}-\mu_iI_{n_g}\end{bmatrix}.$$

Applying the Schur complement to Θ, it can be obtained that $\Theta<0\Leftrightarrow\Theta_1<0$, where

$$\Theta_1=\begin{bmatrix}-F_i+\mu_ic^2\mathcal{I}_x^T\mathcal{I}_x & O & A_{i1}^TF_i-C_{i0}^T\mathcal{F}_i^T\\ \star & -\mu_iI_{n_g} & G_{i1}^TF_i\\ \star & \star & -F_i\end{bmatrix}.\tag{17}$$

Let $L_i=F_i^{-1}\mathcal{F}_i$. It can be shown that the condition (10) can deduce (17), which indicates $\Delta\mathcal{V}_e(k)\le0$. Therefore, estimation error $\mathcal{E}(k)$ is asymptotically stable with $\omega_{ix}(k)=0$.

(ii) In the case of $\omega_{ix}(k)\neq0$, the following auxiliary function is given.

$$\begin{aligned}\mathbb{E}_1=&e_{z_i}(k)^T(k)e_{z_i}(k)-\gamma^2\omega_{ix}^T(k)\omega_{ix}(k)+\Delta\mathcal{V}_e(k)\\ \le&\|e_{z_i}(k)\|_{A_{Li}^TF_iA_{Li}-F_i+I_{n_x+n_{\omega y}+n_a}}^2+2e_{g_i}^T(k)G_{i1}^TF_iA_{Li}e_{z_i}(k)\\ &+2e_{g_i}^T(k)G_{i1}^TF_iD_{i1}\omega_{ix}(k)+\|G_{i1}e_{g_i}(k)\|_{F_i}^2\\ &+\|D_{i1}\omega_{ix}(k)\|_{F_i}^2+2\omega_{ix}^T(k)D_{i1}^TF_iA_{Li}e_{z_i}(k)-\gamma^2\omega_{ix}^T(k)\omega_{ix}(k)\\ \le&\bar{\mathcal{E}}^T(k)\Theta_2\bar{\mathcal{E}}(k),\end{aligned}\tag{18}$$

where $\bar{\mathcal{E}}(k)=\left[e_{z_i}^T(k)\ \ e_{g_i}^T(k)\ \ \omega_{ix}^T(k)\right]^T$, and

$$\Theta_2=\begin{bmatrix}A_{Li}^TF_iA_{Li}-F_i+\mu_ic^2\mathcal{I}_x^T\mathcal{I}_x+I_{n_x+n_{\omega y}+n_a} & A_{Li}^TF_iG_{i1} & A_{Li}^TF_iD_{i1}\\ \star & G_{i1}^TF_iG_{i1}-\mu_iI_{n_g} & G_{i1}^TF_iD_{i1}\\ \star & \star & D_{i1}^TF_iD_{i1}-\gamma^2I_{n_{\omega x}}\end{bmatrix}.$$

Let $L_i=F_i^{-1}\mathcal{F}_i$. Applying the Schur complement to Θ_2, it can be obtained that $\Theta_3<0\Leftrightarrow\Theta_2<0$, where

$$\Theta_3=\begin{bmatrix}-F_i+\mu_ic^2\mathcal{I}_x^T\mathcal{I}_x & O & O & A_{i1}^TF_i-C_{i0}^T\mathcal{F}_i^T\\ \star & -\mu_iI_{n_g} & O & G_{i1}^TF_i\\ \star & \star & -\gamma^2I_{n_{\omega x}} & D_{i1}^TF_i\\ \star & \star & \star & -F_i\end{bmatrix}.\tag{19}$$

Then it can be deduced from (18) that $\Theta_3<0\rightarrow\mathbb{E}_1<0$. It can be shown that (19) is equivalent to condition (10).

Thus, under zero initial condition, it can be obtained from $\Theta_3<0$ that

$$\sum_{k=0}^{\infty}\|e_{z_i}(k)\|^2\le\gamma^2\sum_{k=0}^{\infty}\|\omega_{ix}(k)\|^2.\tag{20}$$

Thus, we can obtain that all the signals of the composite error system (9) are asymptotically stable with the H_∞ performance index γ.

In addition, under nonzero initial conditions, one has

$$\sum_{k=0}^{\infty}\|e_{z_i}(k)\|^2-\gamma^2\sum_{k=0}^{\infty}\|\omega_{ix}(k)\|+\mathcal{V}_e(\infty)-\mathcal{V}_e(0)\le0.\tag{21}$$

According to Assumption 2 and in view that $\mathcal{V}_e$ is positive, it can be inferred that

$$\sum_{k=0}^{\infty}\|e_{z_i}(k)\|^2\le\|e_{z_i}(0)\|_{F_i}^2+\gamma^2\varpi_i.\tag{22}$$

Furthermore, as $\mathcal{V}_e(0)$ is bounded, one has $\lim_{k\rightarrow\infty}e_{z_i}(k)=0$.

By separating the internal structure of the augmented system and the RMO, it can be obtained that

$$\hat{x}_i(k+1)=A_i\hat{x}_i(k)+B_iu_i(k)+G_ig_i(\hat{x}_i(k))+\mathcal{I}_xL_iC_{i0}e_{z_i}(k).\tag{23}$$

The dynamics of the estimated system state are critical in the subsequent controller design because the predictive controller takes the estimated state as the primary input.

3.2. Event-triggered mechanism

As estimation errors and system disturbances are not accessible for the predictive controller, the estimated state trajectories diverge from the predicted state trajectories over each update window. Thus, before the error between the estimated and predicted state trajectory goes too large, an event-triggered mechanism is proposed to confine this error and adjust the frequency of solving the OCP in this subsection.

For the convenience of notation, we introduce two time sequences for the ith agent given by

$\{t_h\}_{h\in\mathbb{N}}$: which denotes the triggering time instants when the OCP is solved and agent i updates its control input.

$\{[t_h]_j\}_{j\in\mathbb{N}_{[1,M]}}$: which denotes the most recent communication time (data package received) of agent j up to the current update time t_h of agent i.

To describe the event-triggered mechanism in the predictive control scheme specifically, dynamics of the estimated system states in the predictive time horizon $s\in\mathbb{N}_{[t_h,t_h+N_p]}$ are represented as

$$\hat{x}_i(s+1|t_h)=A_i\hat{x}_i(s|t_h)+B_i\bar{u}_i(s|t_h)+G_ig_i(\hat{x}_i(s|t_h))+\mathcal{I}_xL_iC_{i0}e_{z_i}(s|t_h),\tag{24}$$

and dynamics of the predictive system are given as

$$\bar{x}_i(s+1|t_h)=A_i\bar{x}_i(s|t_h)+B_i\bar{u}_i(s|t_h)+G_ig_i(\bar{x}_i(s|t_h)).\tag{25}$$

Next, a potential triggering time instant is defined as follows

$$\bar{t}_{h+1}=\inf_{s>t_h}\{s:\|\hat{x}_i(s)-\bar{x}_i(s|t_h)\|\ge\delta_i\},\tag{26}$$

where

$$\delta_i=\sum_{n=0}^{\beta_i-1}(\|A_i\|+\|G_i\|c)^n\|\mathcal{I}_xL_i\|\sqrt{\|e_{y_i}(0)\|_{F_i}^2+\|C_{i0}\|^2\gamma^2\varpi_i},$$

β_i is the adjustable triggering parameter satisfying $\beta_i \in \mathbb{N}_{[1,N_p]}$. The next triggering time instant of t_h is defined as

$$t_{h+1} = \min\{\bar{t}_{h+1}, N_p\}. \tag{27}$$

Lemma 2. *For the nonlinear MAS (1)(a) with Assumptions 1–3 hold, if the event-triggered time sequence $t_h, h \in \mathbb{N}$, is generated as (27), then the lower bound of inter-execution time is given by $\inf_{h\in\mathbb{N}}\{t_{h+1} - t_h\} \geq \beta_i$, and the upper bound is N_p.*

Proof. Consider the difference $\hat{x}_i(t_{h+1}) - \bar{x}_i(t_{h+1}|t_h)$, where $\bar{x}_i(t_{h+1}|t_{h+1}) = \hat{x}_i(t_{h+1})$. Denote $\hat{e}_{x_i}(s) = \hat{x}_i(s) - \bar{x}_i(s|t_h)$. From (24) and (25), it yields

$$\hat{e}_{x_i}(s) = A_i\hat{e}_{x_i}(s-1) + G_i\hat{g}_i(s-1) + \mathcal{I}_x L_i C_{i0} e_{z_i}(s-1), \tag{28}$$

where $\hat{g}_i(s-1) = g_i(\hat{x}_i(s-1)) - g_i(\bar{x}_i(s-1|t_h))$. In the predictive control scheme, we have $\hat{e}_{x_i}(t_h) = \bar{x}_i(t_h|t_h) - \hat{x}_i(t_h) = 0$. Based on (22), one has

$$\begin{aligned}
&\|\hat{e}_{x_i}(s)\| \\
\leq&\|A_i\|\|\hat{e}_{x_i}(s-1)\| + \|G_i\hat{g}_i(s-1)\| + \|\mathcal{I}_x L_i C_{i0} e_{z_i}(s-1)\| \\
\leq&(\|A_i\| + \|G_i\|c)\|\hat{e}_{x_i}(s-1)\| + \|\mathcal{I}_x L_i C_{i0} e_{z_i}(s-1)\| \\
\leq&\chi_i^{s-t_h}\|\hat{e}_{x_i}(t_h)\| + \sum_{n=0}^{s-t_h-1}\chi_i^n\|\mathcal{I}_x L_i C_{i0} e_{z_i}(s-n-1)\| \\
\leq&\sum_{n=0}^{s-t_h-1}\chi_i^n\|\mathcal{I}_x L_i C_{i0} e_{z_i}(s-n-1)\| \\
\leq&\sum_{n=0}^{s-t_h-1}\chi_i^n\|\mathcal{I}_x L_i\|\|C_{i0}\|\sqrt{\|e_{z_i}(0)\|_{F_i}^2 + \gamma^2\varpi_i},
\end{aligned} \tag{29}$$

where $\chi_i = \|A_i\| + \|G_i\|c$. For ease of notation, let $\rho_i = \|\mathcal{I}_x L_i\|\|C_{i0}\|\sqrt{\|e_{z_i}(0)\|_{F_i}^2 + \gamma^2\varpi_i}$. According to the event-triggered mechanism, we have $\|\hat{e}_{x_i}(t_{h+1})\| \geq \delta_i$. According to the triangle inequality property of the matrix norm, one has

$$\sqrt{\|e_{y_i}(0)\|_{F_i}^2 + \|C_{i0}\|^2\gamma^2\varpi_i} \leq \sqrt{\|C_{i0}\|^2\|e_{z_i}(0)\|_{F_i}^2 + \|C_{i0}\|^2\gamma^2\varpi_i}.$$

It can be further induced from (29) that

$$\sum_{n=0}^{\beta_i-1}\chi_i^n\rho_i \leq \|\hat{e}_{x_i}(t_{h+1})\| \leq \sum_{n=0}^{t_{h+1}-t_h-1}\chi_i^n\rho_i, \tag{30}$$

which indicated that $t_{h+1} - t_h \geq \beta_i$. According to (27), the proof is completed.

3.3. Distributed MPC formulation

The control sequence $\{\bar{u}_i(t_h)\}$ in (24) and (25) is obtained by optimizing a cost function in a cooperative way. It means that all agents are dynamically decoupled while the cost function they share is coupled. At time instant t_h, the cost function of each agent is established as

$$\begin{aligned}
&J_i\big(\hat{x}_i(t_h), \tilde{\mathbf{x}}_{\mathbf{j}}(t_h), \bar{\mathbf{u}}_{\mathbf{i}}(t_h)\big) \\
&\triangleq \sum_{s=t_h}^{t_h+N_p-1}\mathcal{L}_i\big(\bar{x}_i(s|t_h), \tilde{x}_j(s|t_h), \bar{u}_i(t_h+s|t_h)\big) + \mathcal{V}_i^f\big(\bar{x}_i(t_h+N_p|t_h)\big),
\end{aligned} \tag{31}$$

where $\mathcal{L}_i$ is the stage cost function, and $\mathcal{V}_i^f$ is the terminal cost function. $\{\bar{x}_i(s|t_h), s \in \mathbb{N}_{[t_h,t_h+N_p]}\}$ is the nominal predicted state trajectory under the predicted control sequence $\bar{\mathbf{u}}_{\mathbf{i}}(t_h) \triangleq \{\bar{u}_i(t_h|t_h), \bar{u}_i(t_h+1|t_h), \ldots, \bar{u}_i(t_h+N_p-1|t_h)\}$. The neighbor state of agent j received by agent i is defined as

$$\tilde{x}_j(s|t_h) = \begin{cases} \bar{x}_j^*(s|[t_h]_j), & s \in \mathbb{N}_{[t_h,[t_h]_j+N_p]}, \\ x_j^K(s|t_h), & s \in \mathbb{N}_{[[t_h]_j+N_p,t_h+N_p-1]}, \end{cases} \tag{32}$$

where $x_j^K(s|t_h) = (A_j + B_jK_j)\tilde{x}_j(s-1|t_h) + G_jg_j\big(\tilde{x}_j(s-1|t_h)\big)$, $\tilde{\mathbf{x}}_{\mathbf{j}}(t_h) \triangleq \{\tilde{x}_j(s|t_h), s \in \mathbb{N}_{[t_h,[t_h]+N_p]}\}$.

The stage cost functions are given as

$$\begin{aligned}
&\mathcal{L}_i\big(\bar{x}_i(s|t_h), \tilde{x}_j(s|t_h), \bar{u}_i(s|t_h)\big) \\
&= \|\bar{x}_i(s|t_h)\|_{Q_i}^2 + \sum_{j\in\mathcal{N}_i}\|\bar{x}_i(s|t_h) - \tilde{x}_j(s|t_h)\|_{Q_{ij}}^2 + \|\bar{u}_i(s|t_h)\|_{R_i}^2,
\end{aligned} \tag{33}$$

where Q_i, Q_{ij}, R_i are positive definite matrices with suitable dimensions. The cooperation term $\sum_{j\in\mathcal{N}_i}\|\bar{x}_i(s|t_h) - \tilde{x}_j(s|t_h)\|_{Q_{ij}}^2$ is to render the state of agent close to its neighbor agent to achieve certain cooperation, which originates from the centralized objective.

The terminal cost function $\mathcal{V}_i^f$ is defined as

$$\mathcal{V}_i^f(t_h) \triangleq \|\bar{x}_i(t_h+N_p|t_h)\|_{P_i}^2, \tag{34}$$

where $P_i > 0$ is with suitable dimensions, which can be obtained from the following lemma. It helps construct a control invariant set of the actual system (1)(a) without system disturbances, which is necessary for dual-mode control in the MPC scheme.

Lemma 3. *With given matrices $Q_i > 0$ and $R_i > 0$, and assume that Assumptions 1–3 hold. Then, there exists a constant $\varepsilon_i > 0$ such that $\Omega_i(\varepsilon_i) \triangleq \{x_i \in \mathbb{R}^{n_i} : \|x_i\|_{P_i}^2 \leq \varepsilon_i^2\}$ is a positively invariant set for MAS (1) with $\omega_{ix}(k) = 0$ under the local control law $u_i(k) = K_ix_i(k) \in \mathcal{U}_i$, $k \geq 0$, if there exists a positive matrix P_i and a positive constant $\tilde{\mu}_i$ such that the following inequality is satisfied.*

$$\begin{bmatrix} -P_i + \tilde{\mu}_i c^2 I_{n_x+n_{\omega y}+n_a} + Q_i + K_i^T R_i K_i & O & A_{Ki}^T P_i \\ \star & -\tilde{\mu}_i I_{n_g} & G_i^T P_i \\ \star & \star & -P_i \end{bmatrix} < 0. \tag{35}$$

Proof. According to Assumption 1, there exists a local control gain matrix K_i such that $A_{Ki} \triangleq A_i + B_iK_i$ is Schur stable. The actual system (1)(a) without disturbances under local state feedback control can be represented as

$$x_i(k+1) = A_{Ki}x_i(k) + G_ig_i\big(x_i(k)\big). \tag{36}$$

Choose Lyapunov function as $\mathcal{V}(x_i(k)) = x_i^T(k)P_ix_i(k)$. To prove the invariant property of $\Omega_i(\varepsilon_i)$, it suffice to prove the following inequality

$$\mathbb{E}_2(k) = \mathcal{V}\big(x_i(k+1)\big) - \mathcal{V}\big(x_i(k)\big) + x_i^T(k)(Q_i + K_i^T R_i K_i)x_i(k) < 0. \tag{37}$$

According to (36) and Lipschitz condition, one has

$$\begin{aligned}
\mathbb{E}_2(k) =& x_i^T(k)[A_{Ki}^T P_i A_{Ki} - P_i + Q_i + K_i^T R_i K_i]x_i(k) \\
&+ 2x_i^T(k)A_{Ki}^T P_i G_i g_i\big(x_i(k)\big) + g_i^T\big(x_i(k)\big)G_i^T P_i G_i g_i\big(x_i(k)\big) \\
\leq& x_i^T(k)[A_{Ki}^T P_i A_{Ki} - P_i + Q_i + K_i^T R_i K_i]x_i(k) \\
&+ 2x_i^T(k)A_{Ki}^T P_i G_i g_i\big(x_i(k)\big) + g_i^T\big(x_i(k)\big)G_i^T P_i G_i g_i\big(x_i(k)\big) \\
&+ \tilde{\mu}_i c^2 x_i^T(k)x_i(k) - \tilde{\mu}_i g_i^T\big(x_i(k)\big)g_i\big(x_i(k)\big) \\
\leq& \tilde{\mathcal{E}}^T(k)\tilde{\Theta}\tilde{\mathcal{E}}(k),
\end{aligned} \tag{38}$$

where $\tilde{\mathcal{E}}(k) = \big[x_i^T(k)\ g_i^T\big(x_i(k)\big)\big]^T$, and

$$\tilde{\Theta} = \begin{bmatrix} A_{Ki}^T P_i A_{Ki} - P_i + \tilde{\mu}_i c^2 I + Q_i + K_i^T R_i K_i & A_{Ki}^T P_i G_i \\ \star & G_i^T P_i G_i - \tilde{\mu}_i I_{n_g} \end{bmatrix}.$$

Applying the Schur complement to $\tilde{\Theta}$, it can be obtained that $\tilde{\Theta} < 0 \Leftrightarrow \tilde{\Theta}_1 < 0$, where

$$\tilde{\Theta}_1 = \begin{bmatrix} -P_i + \tilde{\mu}_i c^2 I_{n_x+n_{\omega y}+n_a} + Q_i + K_i^T R_i K_i & O & A_{Ki}^T P_i \\ \star & -\tilde{\mu}_i I_{n_g} & G_i^T P_i \\ \star & \star & -P_i \end{bmatrix}. \tag{39}$$

The above deduction means $\tilde{\Theta}_1 < 0 \rightarrow \mathbb{E}_2 < 0$. It can be shown that $\tilde{\Theta}_1 < 0$ is equivalent to the condition (35).

Utilizing the designed cost function (31), the OCP of agent i is presented as follows.

$$\mathcal{P}_i(t_h) \triangleq \min_{\bar{\mathbf{u}}_\mathbf{i}(t_h)} J_i\big(\hat{x}_i(t_h), \tilde{\mathbf{x}}_\mathbf{j}(t_h), \bar{\mathbf{u}}_\mathbf{i}(t_h)\big) \tag{40}$$

subject to

$$\bar{x}_i(t_h|t_h) = \hat{x}_i(t_h), \tag{41a}$$

$$\bar{x}_i(s+1|t_h) = A_i\bar{x}_i(s|t_h) + B_i\bar{u}_i(s|t_h) + G_i g_i\big(\bar{x}_i(s|t_h)\big), \tag{41b}$$

$$\|\bar{x}_i(s|t_h)\|_{P_i} \le (t_h + N_p - s + 1)\alpha_i\varepsilon_i, \tag{41c}$$

$$\bar{u}_i(s|t_h) \in \mathcal{U}_i, \tag{41d}$$

where $s \in \mathbb{N}_{[t_h,\ t_h+N_p]}$, $0 < \alpha_i < 1$ is the shrinkage rate to be designed. The solutions of (40) and the corresponding predictive states are denoted as $\bar{\mathbf{u}}_\mathbf{i}^*(t_h)$ and $\bar{\mathbf{x}}_\mathbf{i}^*(t_h)$, respectively.

Remark 3. It is essential to construct a multi-index cost function based on the assumed neighbor states [12,37,38]. The cost function takes the information of the potential neighbor state and the control objective of cooperation into account, which is important for the stability analysis in Section 4.

Remark 4. The novelty of OCP lies in the linear robustness constraints (41c). Compared to [8,9,12], the robustness constraint (41c) inherits the role of being a terminal constraint and innovates the role of decaying the predicted state sequences. The terminal constraint keeps the same as [8], which can still guarantee the cooperation of MAS. Moreover, the inverse proportional process constraints are changed to a linear form, which helps the controller to generate control sequences smoothly. Its efficacy can be illustrated by the comparison between Figs. 7(a) and 7(b) in the simulation results.

The proposed event-triggered DOFMPC scheme of nonlinear MAS synthesizes an attack separable RMO and a designed predictive controller. These components and mechanisms provided an effective predictive control scheme for the cooperation problem of nonlinear MAS. Its overall structure is shown in Fig. 1, and the efficacy of resistance to FDI attacks and disturbances will be provided in Section 4.

4. Recursive feasibility and cooperation

In this section, two important properties of the proposed robust secure DOFMPC scheme, the recursive feasibility of OCP and the cooperation of the nonlinear MAS subject to FDI attacks and disturbances are presented.

4.1. Recursive feasibility

To prove the recursive feasibility of OCP in agent i, we first consider the following candidate solution at t_{h+1}.

$$\bar{\mathbf{u}}_\mathbf{i}(t_{h+1}) = \begin{cases} \bar{u}_i(s|t_h), & s \in \mathbb{N}_{[t_{h+1},\ t_h+N_p-1]}, \\ K_i\bar{x}_i(s|t_{h+1}), & s \in \mathbb{N}_{[t_h+N_p,\ t_{h+1}+N_p-1]}. \end{cases} \tag{42}$$

The difference in predicted nominal state trajectory between two successive computation instants is crucial in the subsequent proof. Its upper bound is given in the following lemma.

Algorithm 1 Event-triggered DOFMPC Algorithm

Offline: Choose proper weighting matrices Q_i and R_i, and find proper local control law K_i by pole assign. Calculate the observation gain matrix L_i by condition (10) in Lemma 1 with given H_∞ performance index γ, and Obtain the weighting matrix P_i by condition (35) in Lemma 3. Choose a proper shrinkage rate α_i, minimum triggering interval β_i satisfy the condition in Theorem 1. Determine cooperation matrices Q_{ij} to satisfy the condition in Theorem 2.

Online:

Step 1:: Set $h = 0$. With initial predicted state equals to observed state $\bar{x}_i(t_0|t_0) = \hat{x}_i(t_0)$. Each agent i solves the OCP $\mathcal{P}_i(t_0)$ by replacing the cooperation term with zero to obtain $\bar{\mathbf{u}}_\mathbf{i}^*(t_0)$ and $\bar{\mathbf{x}}_\mathbf{i}^*(t_0)$.
Then each agent i transmits its predicted state trajectory $\bar{\mathbf{x}}_\mathbf{i}^*(t_0)$ and receive $\bar{\mathbf{x}}_\mathbf{j}^*(t_0)$ from all neighbor agent $j \in \mathcal{N}_i$. Set $s = 0$, and go to Step 3;

For $\hat{x}_i(s) \notin \Omega_i(\alpha_i\varepsilon_i)$ **do**

Step 2: Check event-triggering condition (26). If triggered, go to Step 4. Else, go to Step 3.

Step 3: Apply $\bar{u}_i^*(s|t_h)$ to the ith agent. Set $s = s + 1$.

Step 4: Set $s = t_{h+1}$. Agent i solves the OCP $\mathcal{P}_i(t_{h+1})$ to obtain $\bar{\mathbf{u}}_\mathbf{i}^*(t_{h+1})$ and $\bar{\mathbf{x}}_\mathbf{i}^*(t_{h+1})$, apply $\bar{u}_i^*(t_{h+1}|t_{h+1})$ and transmits its predicted state trajectory to its neighbor agent. Set $s = s + 1$.

Endfor

If $\hat{x}_i(s) \in \Omega_i(\alpha_i\varepsilon_i)$**:** Apply $u_i = K_i\hat{x}_i$ to ith agent.

Lemma 4. *Assume that the control sequence $\bar{\mathbf{u}}_\mathbf{i}(t_h)$ is a feasible solution of $\mathcal{P}_i(t_h)$, and both the actual system and the RMO apply the predicted control sequence $\{\bar{u}_i(t_h|t_h), \bar{u}_i(t_h+1|t_h), \ldots, \bar{u}_i(t_{h+1}-1|t_h)\}$ during the triggering interval. When the tail sequence $\{\bar{u}_i(t_{h+1}|t_h), \ldots, \bar{u}_i(t_h+N_p-1|t_h)\}$ is applied to the predicted system with $\bar{x}_i(t_{h+1}|t_{h+1}) = \hat{x}_i(t_{h+1})$ at the next sampling time t_{h+1}, for $s \in \mathbb{N}_{[t_{h+1},t_h+N_p-1]}$, the difference between the predicted state at time t_{h+1} and the predicted state at time t_h are norm-bounded as follows*

$$\begin{aligned} &\|\bar{x}_i(s|t_{h+1}) - \bar{x}_i(s|t_h)\|_\Omega \\ &\le \begin{cases} \sqrt{\lambda_{\max}(\Omega)}N_p\rho_i, & \text{if} \quad \chi_i = 1, \\ \chi_i^{s-t_{h+1}}\sqrt{\lambda_{\max}(\Omega)}\dfrac{1-\chi_i^{N_p}}{1-\chi_i}\rho_i, & \text{if} \quad \chi_i \ne 1. \end{cases} \end{aligned} \tag{43}$$

Proof. Following the dynamics (41b), for $s \in \mathbb{N}_{[t_{h+1},t_h+N_p]}$, the predicted states at time t_{h+1} and t_h are given as

$$\bar{x}_i(s|t_{h+1}) = A_i\bar{x}_i(s-1|t_{h+1}) + B_i\bar{u}_i(s-1|t_{h+1}) + G_i g_i\big(\bar{x}_i(s-1|t_{h+1})\big), \tag{44}$$

$$\bar{x}_i(s|t_h) = A_i\bar{x}_i(s-1|t_h) + B_i\bar{u}_i(s-1|t_h) + G_i g_i\big(\bar{x}_i(s-1|t_h)\big). \tag{45}$$

For convenience of notation, we denote $\bar{e}_{x_i}(s) = \bar{x}_i(s|t_{h+1}) - \bar{x}_i(s|t_h)$. According to the assumption that $\bar{u}_i(s|t_{h+1}) = \bar{u}_i(s|t_h)$, $s \in \mathbb{N}_{[t_{h+1},t_h+N_p-1]}$, and the triangle inequality and Lipschitz assumption, the difference can be deduced as

$$\begin{aligned} \|\bar{e}_{x_i}(s)\| &= \|A_i\bar{e}_{x_i}(s-1) + G_i\Big(g_i\big(\bar{x}_i(s-1|t_{h+1})\big) - g_i\big(\bar{x}_i(s-1|t_h)\big)\Big)\| \\ &\le \|A_i\bar{e}_{x_i}(s-1)\| + c\|G_i\|\|\bar{e}_{x_i}(s-1)\| \\ &\le \chi_i\|\bar{e}_{x_i}(s-1)\| \\ &\le \chi_i^{s-t_{h+1}}\|\bar{e}_{x_i}(t_{h+1})\|. \end{aligned} \tag{46}$$

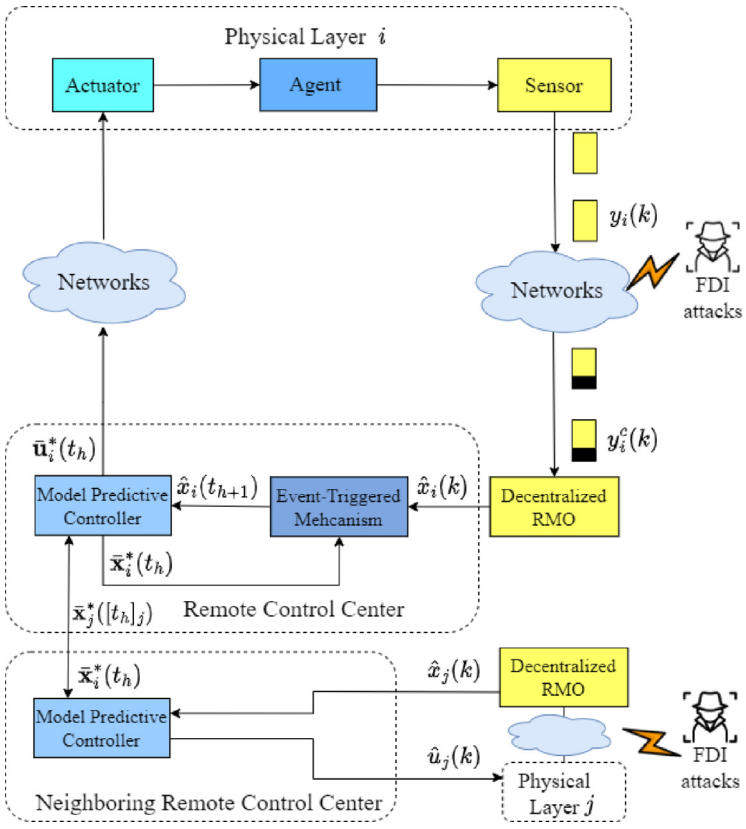

Fig. 1. Control framework of event-triggered DOFMPC in nonlinear MAS.

According to (41a), one has $\bar{e}_{x_i}(t_{h+1}) = \hat{e}_{x_i}(t_{h+1})$. It can be obtained from (30) and $t_{h+1} - t_h \le N_p$ that

$$\begin{aligned}\|\bar{x}_i(s|t_{h+1}) - \bar{x}_i(s|t_h)\|_\Omega &\le \chi_i^{s-t_{h+1}}\sqrt{\lambda_{\max}(\Omega)}\|\hat{e}_{x_i}(t_{h+1})\| \\ &\le \chi_i^{s-t_{h+1}}\sqrt{\lambda_{\max}(\Omega)}\sum_{n=0}^{t_{h+1}-t_h-1}\chi_i^n\rho_i \\ &\le \begin{cases}\sqrt{\lambda_{\max}(\Omega)}N_p\rho_i, & \text{if} \quad \chi_i = 1, \\ \chi_i^{s-t_{h+1}}\sqrt{\lambda_{\max}(\Omega)}\dfrac{1-\chi_i^{N_p}}{1-\chi_i}\rho_i, & \text{if} \quad \chi_i \ne 1,\end{cases}\end{aligned} \tag{47}$$

which completes the proof.

Based on the upper bound of successive predicted nominal state trajectory differences, the recursive feasibility of OCP is given in the following theorem.

Theorem 1. *For the OCP $\mathcal{P}_i(t_h)$ of agent i, supposing that Assumptions 1–3 hold and the initial OCP $\mathcal{P}_i(t_0)$ is feasible, and assuming that $\bar{\mathbf{u}}_i(t_h) = \{\bar{u}_i(t_h|t_h), \bar{u}_i(t_h+1|t_h), \ldots, \bar{u}_i(t_h+N_p-1|t_h)\}$ is a feasible solution at time t_h, then it holds that $\mathcal{P}_i(t_{h+1})$ is feasible at time t_{h+1}, if the following conditions are satisfied: (a) The initial observer error $e_{z_i}(0)$ and the energy bound of system disturbances ϖ_i satisfy:*

$$\sqrt{\|e_{z_i}(0)\|_{F_i}^2 + \gamma^2\varpi_i}$$

$$\le \begin{cases}\dfrac{(1-\alpha_i)(1-\chi_i)\varepsilon_i}{\sqrt{\lambda_{\max}(P_i)}(1-\chi_i^{N_p})\|\mathcal{I}_x L_i\|\|C_{i0}\|}, & \text{if } \chi_i < 1, \\ \dfrac{(1-\alpha_i)\varepsilon_i}{\sqrt{\lambda_{\max}(P_i)}N_p\|\mathcal{I}_x L_i\|\|C_{i0}\|}, & \text{if } \chi_i = 1, \\ \dfrac{(1-\alpha_i)(1-\chi_i)\varepsilon_i}{\sqrt{\lambda_{\max}(P_i)}(1-\chi_i^{N_p})\chi^{N_p-\beta_i}\|\mathcal{I}_x L_i\|\|C_{i0}\|}, & \text{if } \chi_i > 1.\end{cases} \tag{48}$$

(b) The shrinkage rate α_i satisfies:

$$\alpha_i \ge 1 - \sqrt{\frac{\lambda_{\min}(Q_i + K_i^T R_i K_i)}{\lambda_{\max}(P_i)}}. \tag{49}$$

(c) The minimum triggering β_i satisfies :

$$\beta_i \ge \frac{1}{\alpha_i} - 1. \tag{50}$$

In addition, the OCP $\mathcal{P}_i(t_h)$ is feasible for all time $\{t_h\}$.

Proof. By splitting the prediction horizon into three parts based on one terminal point $t_h + N_p$, we can prove the feasibility orderly.

(1) Time interval $\{t_{h+1}, \ldots, t_h + N_p - 1\}$: according to constraints (41c), we have

$$\|\bar{x}_i(s|t_h)\|_{P_i} \le (t_h + N_p - s + 1)\alpha_i\varepsilon_i. \tag{51}$$

To satisfy the robustness constraint (41c) for $\bar{x}_i(s|t_{h+1})$, it suffices to prove that $\|\bar{x}_i(s|t_{h+1}) - \bar{x}_i(s|t_h)\|_{P_i} \le (t_{h+1} - t_h)\alpha_i\varepsilon_i$. To that end, we analyze it from the following three cases with Lemma 4, condition (a) and (c):

Case 1: if $\chi_i = 1$, one has

$$\begin{aligned}\|\bar{x}_i(s|t_{h+1}) - \bar{x}_i(s|t_h)\|_{P_i} \leq & \sqrt{\lambda_{\max}(P_i)} N_p \|\mathcal{I}_x L_i\| \|C_{i0}\| \sqrt{\|e_{z_i}(0)\|^2_{F_i} + \gamma^2 \varpi_i} \\ \leq & (1-\alpha_i)\varepsilon_i \\ \leq & (t_{h+1} - t_h)\alpha_i \varepsilon_i. \end{aligned} \tag{52}$$

Case 2: if $\chi_i > 1$, it yields from $t_{h+1} - t_h \geq \beta_i$ and (43) that

$$\begin{aligned}\|\bar{x}_i(s|t_{h+1}) - \bar{x}_i(s|t_h)\|_{P_i} \leq & \chi_i^{s-t_{h+1}} \sqrt{\lambda_{\max}(P_i)} \frac{1-\chi_i^{N_p}}{1-\chi_i} \rho_i \\ \leq & \chi_i^{t_h+N_p-t_{h+1}} \sqrt{\lambda_{\max}(P_i)} \frac{1-\chi_i^{N_p}}{1-\chi_i} \rho_i \\ \leq & \chi_i^{N_p-\beta_i} \sqrt{\lambda_{\max}(P_i)} \frac{1-\chi_i^{N_p}}{1-\chi_i} \rho_i \\ \leq & (1-\alpha_i)\varepsilon_i \\ \leq & (t_{h+1} - t_h)\alpha_i \varepsilon_i. \end{aligned} \tag{53}$$

Case 3: if $\chi_i < 1$, we have

$$\begin{aligned}\|\bar{x}_i(s|t_{h+1}) - \bar{x}_i(s|t_h)\|_{P_i} \leq & \chi_i^{s-t_{h+1}} \sqrt{\lambda_{\max}(P_i)} \frac{1-\chi_i^{N_p}}{1-\chi_i} \rho_i \\ \leq & \sqrt{\lambda_{\max}(P_i)} \frac{1-\chi_i^{N_p}}{1-\chi_i} \rho_i \\ \leq & (1-\alpha_i)\varepsilon_i \\ \leq & (t_{h+1} - t_h)\alpha_i \varepsilon_i. \end{aligned} \tag{54}$$

From triangle inequality, the candidate predicted state trajectory under $\bar{\mathbf{u}}_i(t_{h+1})$ can be inferred as

$$\begin{aligned}\|\bar{x}_i(s|t_{h+1})\|_{P_i} \leq & \|\bar{x}_i(s|t_h)\|_{P_i} + \|\bar{x}_i(s|t_{h+1}) - \bar{x}_i(s|t_h)\|_{P_i} \\ \leq & (t_{h+1} + N_p - s + 1)\alpha_i \varepsilon_i. \end{aligned} \tag{55}$$

So the robust constraints (41c) in $\mathcal{P}_i(t_{h+1})$ are satisfied in $[t_{h+1},\ t_h + N_p]$. The associate candidate solution $\{\bar{u}_i(s|t_{h+1})\}$ keeps the same as the feasible solution $\bar{\mathbf{u}}_i(t_h)$, so that control constraints (41d) are obviously satisfied.

(2) In particular, the predictive terminal time point satisfies $\|\bar{x}_i(t_h + N_p|t_h)\|_{P_i} \leq \alpha_i \varepsilon_i$, and $\|\bar{x}_i(s|t_{h+1}) - \bar{x}_i(s|t_h)\|_{P_i} \leq (1-\alpha_i)\varepsilon_i$, so it is easy to obtained that $\|\bar{x}_i(t_h + N_p|t_{h+1})\|_{P_i} \leq \varepsilon_i$.

(3) Time interval $\{t_h + N_p, \ldots, t_{h+1} + N_p\}$: The candidate solution (42) $\bar{u}_i(s|t_{h+1}) = K_i(\bar{x}_i(s|t_{h+1})) \in \mathcal{U}_i$ implies that control constraints (41d) are satisfied. From Lemma 2 and condition (b), we have

$$\begin{aligned}&\|\bar{x}_i(s+1|t_{h+1})\|_{P_i} \\ &< \|\bar{x}_i(s|t_{h+1})\|_{P_i} - \sqrt{\bar{x}_i(s|t_{h+1})^T (Q_i + K_i^T R_i K_i) \bar{x}_i(s|t_{h+1})} \\ &< \Big(1 - \sqrt{\frac{\lambda_{\min}(Q_i + K_i^T R_i K_i)}{\lambda_{\max}(P_i)}}\Big) \|\bar{x}_i(s-1|t_{h+1})\|_{P_i} \\ &< \Big(1 - \sqrt{\frac{\lambda_{\min}(Q_i + K_i^T R_i K_i)}{\lambda_{\max}(P_i)}}\Big)^{s-t_h-N_p+1} \|\bar{x}_i(t_h + N_p|t_{h+1})\|_{P_i} \\ &< \alpha_i \varepsilon_i \\ &< (t_{h+1} + N_p - s + 1)\alpha_i \varepsilon_i. \end{aligned} \tag{56}$$

The robustness constraints (41c) in $\mathcal{P}_i(t_{h+1})$ are satisfied. With the initial feasibility assumption, according to the mathematical induction, it can be concluded that the OCP $\mathcal{P}_i(t_h)$ is recursively feasible for all time $\{t_h\}$. The above analysis completes the proof.

Remark 5. The conditions on the initial estimation error are general in the stability analysis of the OFMPC [25,37,39]. In contrast to the conventional MPC, output feedback MPC generates effective control inputs using estimated states rather than measured states. If the constraint on initial estimation error is not taken into account, the estimated state could be unreliable to generate effective control inputs. To guarantee the satisfaction of original constraints, it is crucial and appropriate to constrain the initial estimation error.

4.2. Cooperation

To prove the cooperation of the proposed event-triggered DOFMPC scheme in the MAS subject to FDI attacks and disturbances, the following lemma is presented firstly to guarantee the reachability of terminal constraints for the estimated states.

Lemma 5. *For the nonlinear MAS (1)(a), supposing that Assumptions 1–3 hold and the initial OCP $\mathcal{P}_i(t_0)$ is feasible, then the estimated states of the ith agent $\hat{x}_i$ will enter $\Omega_i(\varepsilon_i)$ in finite time if the cooperation matrices Q_{ij} satisfy*

$$\begin{aligned}&\sum_{j\in\mathcal{N}_i} \lambda_{\max}(Q_{ij}) \left(\frac{\alpha_i^2 \varepsilon_i^2}{\lambda_{\min}(P_i)} + \frac{\alpha_j^2 \varepsilon_j^2}{\lambda_{\min}(P_j)} \right) \\ &\quad \leq \frac{6 \frac{\lambda_{\max}(Q_i)}{\lambda_{\min}(P_i)} \beta_i^2 \left[\varepsilon_i^2 - \lambda_{\max}(Q_i)\delta_i^2 - (N_p - \beta_i)\alpha_i^2 \varepsilon_i^2 \right] - (1-\alpha_i)^2 \varepsilon_i^2}{2N_p{}^3 + 9N_p{}^2 + 13N_p}. \end{aligned} \tag{57}$$

Proof. Following the dynamics of predictive system (25) and Lemma 5, one has

$$\begin{aligned}&\bar{J}_i(t_{h+1}) - J_i^*(t_h) \\ &= \sum_{s=t_{h+1}}^{t_{h+1}+N_p-1} \Big\{ \|\bar{x}_i(s|t_{h+1})\|^2_{Q_i} + \|\bar{u}_i(s|t_{h+1})\|^2_{R_i} \\ &\quad + \sum_{j\in\mathcal{N}_i} \|\bar{x}_i(s|t_{h+1}) - \tilde{x}_j(s|t_{h+1})\|^2_{Q_{ij}} \Big\} \\ &\quad - \sum_{s=t_h}^{t_h+N_p-1} \Big\{ \|\bar{x}_i(s|t_h)^*\|^2_{Q_i} + \|\bar{u}_i^*(s|t_h)\|^2_{R_i} \\ &\quad + \sum_{j\in\mathcal{N}_i} \|\bar{x}_i^*(s|t_h) - \tilde{x}_j(s|t_h)\|^2_{Q_{ij}} \Big\} \\ &\quad + \|\bar{x}_i(t_{h+1} + N_p|t_{h+1})\|^2_{P_i} - \|\bar{x}_i(t_h + N_p|t_h)\|^2_{P_i} \\ &= \Delta_{J_1} + \Delta_{J_2} + \Delta_{J_3} + \Delta_{J_4}, \end{aligned} \tag{58}$$

where

$$\begin{aligned}\Delta_{J_1} = & -\sum_{s=t_h}^{t_{h+1}-1} \Big\{ \|\bar{x}_i(s|t_h)^*\|^2_{Q_i} + \|\bar{u}_i^*(s|t_h)\|^2_{R_i} \\ & + \sum_{j\in\mathcal{N}_i} \|\bar{x}_i^*(s|t_h) - \tilde{x}_j(s|t_h)\|^2_{Q_{ij}} \Big\}, \end{aligned}$$

$$\begin{aligned}\Delta_{J_2} = & \sum_{s=t_{h+1}}^{t_h+N_p-1} \Big\{ \|\bar{x}_i(s|t_{h+1})\|^2_{Q_i} - \|\bar{x}_i(s|t_h)^*\|^2_{Q_i} \\ & + \|\bar{u}_i(s|t_{h+1})\|^2_{R_i} - \|\bar{u}_i(s|t_h)\|^2_{R_i} \Big\}, \end{aligned}$$

$$\begin{aligned}\Delta_{J_3} = & \sum_{s=t_{h+1}}^{t_h+N_p-1} \sum_{j\in\mathcal{N}_i} \Big\{ \|\bar{x}_i(s|t_{h+1}) - \tilde{x}_j(s|t_{h+1})\|^2_{Q_{ij}} \\ & - \|\bar{x}_i^*(s|t_h) - \tilde{x}_j(s|t_h)\|^2_{Q_{ij}} \Big\} \end{aligned}$$

$$+\sum_{s=t_h+N_p}^{t_{h+1}+N_p-1}\left\{\sum_{j\in\mathcal{N}_i}\|\bar{x}_i(s|t_{h+1})-\tilde{x}_j(s|t_{h+1})\|^2_{Q_{ij}}\right\},$$

$$\Delta_{J_4}=\sum_{s=t_h+N_p}^{t_{h+1}+N_p-1}\left\{\|\bar{x}_i(s|t_{h+1})\|^2_{Q_i}+\|\bar{u}_i(s|t_{h+1})\|^2_{R_i}\right\}$$
$$+\|\bar{x}_i(t_{h+1}+N_p|t_{h+1})\|^2_{P_i}-\|\bar{x}_i(t_h+N_p|t_h)\|^2_{P_i}.$$

Next, we analyze each term orderly. From the event-triggered mechanism, one has

$$\|\bar{x}_i(s|t_h)^*\|^2_{Q_i}\geq\|\hat{x}_i(s|t_h)^*\|^2_{Q_i}-\|\hat{e}_{x_i}(s)\|^2_{Q_i}\geq\varepsilon_i^2-\lambda_{\max}(Q_i)\delta_i^2.$$

Then we have

$$\Delta_{J_1}\leq-\sum_{s=t_h}^{t_{h+1}-1}\left\{\|\bar{x}_i(s|t_h)^*\|^2_{Q_i}\right\}$$
$$\leq-\frac{\lambda_{\max}(Q_i)}{\lambda_{\min}(P_i)}\beta_i^2\left(\varepsilon_i^2-\lambda_{\max}(Q_i)\delta_i^2\right). \tag{59}$$

Second, from (46), (51) and Theorem 1, using triangle equality, one has

$$\Delta_{J_2}=\sum_{s=t_{h+1}}^{t_h+N_p-1}\left\{\|\bar{x}_i(s|t_{h+1})\|^2_{Q_i}-\|\bar{x}_i(s|t_h)^*\|^2_{Q_i}\right\}$$
$$\leq\sum_{s=t_{h+1}}^{t_h+N_p-1}\left\{\|\bar{x}_i(s|t_{h+1})-\bar{x}_i(s|t_h)^*\|^2_{Q_i}\right\}$$
$$\leq\frac{\lambda_{\max}(Q_i)}{\lambda_{\min}(P_i)}\sum_{s=t_{h+1}}^{t_h+N_p-1}\beta_i^2\alpha_i^2\varepsilon_i^2$$
$$\leq\frac{\lambda_{\max}(Q_i)}{\lambda_{\min}(P_i)}(N_p-\beta_i)\beta_i^2\alpha_i^2\varepsilon_i^2. \tag{60}$$

Third, from the definition of the neighbor term, one has

$$\Delta_{J_3}\leq\sum_{s=t_{h+1}}^{t_{h+1}+N_p-1}\sum_{j\in\mathcal{N}_i}\left\{\|\bar{x}_i(s|t_{h+1})\|^2_{Q_{ij}}+\|\tilde{x}_j(s|t_{h+1})\|^2_{Q_{ij}}\right\}$$
$$\leq\sum_{s=t_{h+1}}^{t_{h+1}+N_p-1}\sum_{j\in\mathcal{N}_i}\left\{\frac{\lambda_{\max}(Q_{ij})}{\lambda_{\min}(P_i)}(t_{h+1}+N_p-s+1)^2\alpha_i^2\varepsilon_i^2\right.$$
$$\left.+\frac{\lambda_{\max}(Q_{ij})}{\lambda_{\min}(P_j)}(t_{h+1}+N_p-s+1)^2\alpha_j^2\varepsilon_j^2\right\}$$
$$\leq\sum_{n=2}^{N_p+1}\sum_{j\in\mathcal{N}_i}\left\{\frac{\lambda_{\max}(Q_{ij})}{\lambda_{\min}(P_i)}n^2\alpha_i^2\varepsilon_i^2+\frac{\lambda_{\max}(Q_{ij})}{\lambda_{\min}(P_j)}n^2\alpha_j^2\varepsilon_j^2\right\}$$
$$\leq\sum_{n=2}^{N_p+1}n^2\sum_{j\in\mathcal{N}_i}\lambda_{\max}(Q_{ij})\left\{\frac{\alpha_i^2\varepsilon_i^2}{\lambda_{\min}(P_i)}+\frac{\alpha_j^2\varepsilon_j^2}{\lambda_{\min}(P_j)}\right\}. \tag{61}$$

Lastly, according to Lemma 2, we have $\Delta_{J_4}\leq\|\bar{x}_i(t_h+N_p|t_{h+1})\|^2_{P_i}-\|\bar{x}_i(t_h+N_p|t_h)\|^2_{P_i}\leq(1-\alpha_i)^2\varepsilon_i^2$. Under condition (57), it suffices to prove that $\Delta_{J_1}+\Delta_{J_2}+\Delta_{J_3}+\Delta_{J_4}\leq 0$. Summarizing all the above discussion, one has

$$\bar{J}_i^*(t_{h+1})-J_i^*(t_h)\leq\bar{J}_i(t_{h+1})-J_i^*(t_h)\leq 0. \tag{62}$$

According to the same arguments in [40,41], it can be shown that the estimated state of each agent enters the terminal set $\Omega_i(\varepsilon_i)$ in finite time.

Remark 6. In order to accomplish the control goal of the cooperation, a cooperation term is added to the predictive controller. However, the cooperation term appearing in the objective function poses difficulties in the proof of stability for nonlinear MAS. To handle it, we take full advantage of the definition of the assumed neighbor states (32) and the satisfaction of the terminal constraints (41c) in Eq. (61). With the elaborate design of the cooperation term, the cooperation of the nonlinear MAS can be proved by selecting a suitable cooperation matrix Q_{ij}.

Now the cooperation of nonlinear MAS can be achieved by summarizing all the above discussions, which are concluded in the following theorem.

Theorem 2. *For the nonlinear MAS (1)(a) with S–C FDI attacks and disturbances, supposing that Assumptions 1–3 hold and the initial OCP $\mathcal{P}_i(t_0)$ is feasible if the conditions in Theorem 1 and Lemma 5 hold, then the system state of all agent will cooperatively asymptotically stabilize to the origin under the proposed event-triggered DOFMPC Algorithm 1.*

Proof. Firstly, according to Lemma 1, one has $\lim_{k\to\infty}e_{zi}(k)=0$. There exists a finite time instant $\bar{k}$ such that $\sqrt{\lambda_{\max}(P_i)}\ \|\mathcal{I}_x L_i C_{i0}\ e_{zi}(k)\|\leq(1-\alpha_i)\varepsilon_i,\ \forall\ k>\bar{k}$. Furthermore, according to Lemma 5, the estimated state satisfies $\hat{x}_i(k)\in\Omega_i(\varepsilon_i)$ eventually. It is obviously that we can seek a constant $k'>\bar{k}$, such that $\|\hat{x}_i(k')\|_{P_i}\leq\varepsilon_i$.

Then under Algorithm 1, local state-feedback control sequences $u_i(k)=K_i x_i(k), k\geq k'$ are applied to both the RMO and the actual system. Induced from Lemma 3 and (23), one has $\mathcal{V}\big(\hat{x}_i(k+1)\big)<\mathcal{V}\big(\hat{x}_i(k)\big)-\hat{x}_i^T(k)(Q_i+K_i^T R_i K_i)\ \hat{x}_i(k)+\sqrt{\lambda_{\max}(P_i)}\|\mathcal{I}_x L_i C_{i0} e_{zi}(k)\|$. As mentioned above, it can be obtained from condition (b) in Theorem 1 that $\|\hat{x}_i(k)\|_{P_i}\leq\alpha_i\|\hat{x}_i(k-1)\|_{P_i}+(1-\alpha_i)\varepsilon_i$. It implies the estimated state cannot escape from $\Omega_i(\varepsilon_i)$, $\forall\ k>k'$.

Furthermore, we have $\|\hat{x}_i(k)\|_{P_i}\leq(\alpha_i)^{k-k'}\varepsilon_i+\sum_{n=k'}^{k}(\alpha_i)^n\sqrt{\lambda_{\max}(P_i)}\|\mathcal{I}_x L_i C_{i0} e_{zi}(k)\|, \forall\ k>k'$. As $0<\alpha_i<1$ and $\lim_{k\to\infty}e_{zi}(k)=0$, one has $\lim_{k\to\infty}\hat{x}_i(k)=0$. Recalling the conclusion $\lim_{k\to\infty}e_{zi}(k)=0$ in Lemma 1, we have $\lim_{k\to\infty}x_i(k)=0$.

Summarizing all the above discussions, similar to [8], it proves the stability of each agent and the cooperation of the overall nonlinear MAS subject to FDI attacks and external disturbances can be achieved under Algorithm 1.

5. Simulation

The simulation example is a typical nonlinear one-link flexible joint manipulator system, in which a linear torsional spring is used to simulate the joint's elasticity [42]. Consider the simulation experiment scenario: The two pairs of operators cooperate to achieve stability. Their communication topology is quadrilateral, and the unpaired agents are connected. The dynamics of each agent are modeled as

$$\begin{cases}\dot{\theta}_m=w_m,\\ \dot{w}_m=\dfrac{j}{k_m}(\theta_l-\theta_m)-\dfrac{v}{k_m}w_m+\dfrac{U}{k_m}u,\\ \dot{\theta}_l=w_l,\\ \dot{w}_l=\dfrac{j}{k_l}(\theta_m-\theta_l)-\dfrac{M}{k_l}sin(\theta_l),\end{cases} \tag{63}$$

where $\theta_m, w_m, \theta_l, w_l$ are motor rotor rotation angles, motor rotor angular velocity, link rotation angles, and link angular velocity, respectively. The system parameter k_m, k_l, j, v, and M represent the motor rotor inertia, link inertia, joint elastic constant, viscous friction, and gravitational parameter, respectively.

By linearizing and selecting an appropriate sampling interval, the system dynamic (63) with disturbances and FDI attacks can

be represented by (1)(a). We get the following matrices for each agent.

$$A_{1,3}=\begin{bmatrix}0.1974 & 0.0102 & 0.0026 & 0\\ -0.2967 & 0.2847 & 0.2967 & 0.0026\\ 0.0001 & 0 & 0.1999 & 0.0103\\ 0.0201 & 0.0001 & -0.0106 & 0.1999\end{bmatrix},$$

$$A_{2,4}=\begin{bmatrix}0.2974 & 0.0302 & 0.0036 & 0\\ -0.3967 & 0.1847 & 0.3967 & 0.0029\\ 0.0001 & 0 & 0.1789 & 0.0106\\ 0.0303 & 0.0001 & -0.0106 & 0.6999\end{bmatrix},$$

$$B_{1,3}=\begin{bmatrix}0\\ 0.2160\\ 0\\ 0\end{bmatrix},$$

$$B_{2,4}=\begin{bmatrix}0\\ 0.3160\\ 0\\ 0\end{bmatrix}, G_{1,2,3,4}=\begin{bmatrix}0\\ 0\\ 0\\ -0.0033\end{bmatrix},$$

$$D_{x1,2,3,4}=\begin{bmatrix}0.1\\ 0\\ 0\\ 0\end{bmatrix}, D_{y1,2,3,4}=\begin{bmatrix}0.1\\ -0.1\\ 0.2\\ 0\end{bmatrix},$$

$$S_{1,2,3,4}=\begin{bmatrix}0.1\\ 0.2\\ -0.1\\ 0\end{bmatrix}.$$

The output matrices are $C_{1,2,3,4}=I_4$, and Lipschitz constants are $c_{1,2,3,4}=0.2$. The dynamics of the measurement disturbances consist of a number of segmented trigonometric functions, whose specific values can be seen in Fig. 5(b). We assume the S–C FDI attacks are $a_{1y}(k)=0$ for $k\le 5$, $a_{1y}(k)=sin(3k-2)+cos(5k)$ for $5<k\le 10$, $a_{1y}(k)=0$ for $10<k\le 18$, $a_{1y}(k)=sin(2k+2)$ for $18<k\le 25$, and $a_{1y}(k)=0.8$ for $25<k\le 30$. S–C FDI attacks of other agents are similar and will not be detailed here. The system disturbances are energy bounded as $\omega_{1x}=e^{-4k}sin(3k)$, $\omega_{2x}=e^{-k}sin(3k)$, $\omega_{3x}=e^{-2k}sin(3k)$, and $\omega_{4x}=e^{-2k}sin(1.8k)$. The system control constraints are $\{|u_{1,2,3,4}(k)|\le 2\}$.

Set the weight matrices as $Q_{1,3}=diag(1.31,\ 1.12,\ 1.22,\ 1.23)$ $Q_{2,4}=diag(0.68,\ 0.72,\ 0.72,\ 0.68)$ and $R_{1,2,3,4}=0.01$. The H_∞ performance index $\gamma=2$.

According to the offline procedure in Algorithm 1, the observation matrices and control matrices are obtained from Lemma 1, 3 as follows.

$$L_{1,3}=\begin{bmatrix}-0.3034 & -0.5115 & -0.4648 & 0.0209\\ -0.3484 & -0.4991 & 0.3370 & 0\\ -0.3404 & 0.4254 & -0.4100 & -0.0098\\ -0.0030 & 0.0040 & 0.0047 & 0.1999\\ -0.0642 & 0.0783 & -0.1717 & 0.0002\\ -0.0819 & -0.1793 & 0.0772 & 0\end{bmatrix},$$

$$L_{2,4}=\begin{bmatrix}-0.2031 & -5739 & -0.5125 & 0.0313\\ -0.3040 & -0.6269 & 0.3393 & 0.0004\\ -0.3444 & 0.4884 & -0.3888 & -0.0098\\ -0.0030 & 0.0040 & 0.0049 & 0.6999\\ -0.0598 & 0.0943 & -0.1749 & 0.0002\\ -0.0805 & -0.2004 & 0.0866 & 0.0001\end{bmatrix},$$

$$P_{1,3}=\begin{bmatrix}3.1051 & 0.1027 & 0.0189 & 0.2340\\ 0.1027 & 2.5390 & 0.1702 & 0.0544\\ 0.0189 & 0.1702 & 3.3061 & -0.1363\\ 0.2340 & 0.0544 & -0.1363 & 3.3329\end{bmatrix},$$

$$P_{2,4}=\begin{bmatrix}1.6232 & 0.0311 & 0.0115 & 0.0223\\ 0.0311 & 1.5942 & 0.0231 & 0.0256\\ 0.0115 & 0.0231 & 1.6330 & 0.0180\\ 0.0223 & 0.0256 & 0.0180 & 1.6168\end{bmatrix},$$

$$K_{1,3}=\begin{bmatrix}2.0699 & -0.8797 & -3.2901 & 1.8587\end{bmatrix},$$

$$K_{2,4}=\begin{bmatrix}1.4588 & 0.0213 & -1.1991 & -0.0633\end{bmatrix},$$

According to Theorem 1, the shrinkage rate are chosen as $\alpha_{1,2,3,4}=0.48$, and the triggering parameters are select as $\beta_{1,2,3,4}=2$. Assume that the initial states of manipulator are taken as $x_1(0)=[-16;-8;-14;10]$, $x_2(0)=[14;-14;16;-18]$, $x_3(0)=[-12;-12;-16;17]$, $x_4(0)=[-14;-8;-12;18]$, and the initial values of estimator are chosen as $z_1(0)=[-15.5;-7.09;-13.01;9.93;0;0]$, $z_2(0)=[14.14;-14.35;16.46;-17.19;0;0]$, $z_3(0)=[-11.79;-12.02;-15.84;17.98;0;0]$, $z_4(0)=[-14.44;-7.26;-11.441;17.31;0;0]$. Obviously, they satisfy condition (a) in Theorem 1. Furthermore, cooperation matrices are calculate as $Q_{12,14,32,34}=diag([2.3152\ 1.9366\ 1.9423\ 2.1319])$, and $Q_{12,14,32,34}=diag([1.2694\ 1.3463\ 1.1107\ 1.1639])$, which also satisfy condition in Theorem 2. The event-triggered DOFMPC Algorithm 1 with prediction horizon $N_p=8$ is applied to the nonlinear MAS. For ease of notation, $(a_i)_b$ in the simulation results denotes the bth dimensional component of the vector a_i (see Fig. 2).

In this paper, the event-triggered DOFMPC scheme is proposed to resist initial bounded FDI attacks in the S–C channel, measurement disturbances, and energy-bounded system disturbances in the nonlinear MAS. In terms of structure, an RMO is first built to get valuable information through the compromised outputs, which can estimate uncompromised system states, S–C FDI attacks, and measurement disturbances simultaneously. Therefore, the real-time estimation results of the RMO are first analyzed as follows.

The estimation error of the uncompromised state and output are shown in Figs. 2 and 3. It implies each component of the estimation error rapidly converges to zero after a small initial step. The H_∞ performance of RMO is shown in Fig. 4. Specifically, the estimations of FDI attacks $\hat{a}_i$ converge to the real FDI attacks a_i, which can be illustrated by the light turquoise dotted lines that coincide with the deep green solid lines in Fig. 5(a). Measurement disturbances and their estimations of all agents after the attack are illustrated with brick red solid lines and light blue dashed lines in Fig. 5(b). All the estimation results demonstrate that the observation errors of RMO converge to zero and the uncompromised states, measurement disturbances, and FDI attacks are eventually approximated from augmented states and segregated. It further demonstrates the RMO eliminated the impact of FDI attacks.

The actual system state trajectories of agents are presented in Fig. 6, which reveals that the states converge to zero under event-triggered DOFMPC within the predictive time domain. More specifically, as illustrated by motor rotor angular velocity trajectories, the neighboring agents will cooperatively stabilize to zero, which is related to the cooperation matrix of cost functions in OCP.

Conformed to the saturation of the actuator, the input constraints $\{|u_{1,2,3,4}(k)|\le 2\}$ are strictly satisfied for all agents as shown in Fig. 7(a). The newly-designed robustness constraint results in a smoother predictive control sequence with less oscillation, as can be seen from the comparison in Fig. 7(a) and Fig. 7(b).

Fig. 8 displayed the triggering times and intervals of the event-triggered DOFMPC in the prediction time domain. As we can observe, the triggering intervals steadily lengthen as the system disturbance continues to diminish, which is consistent with the

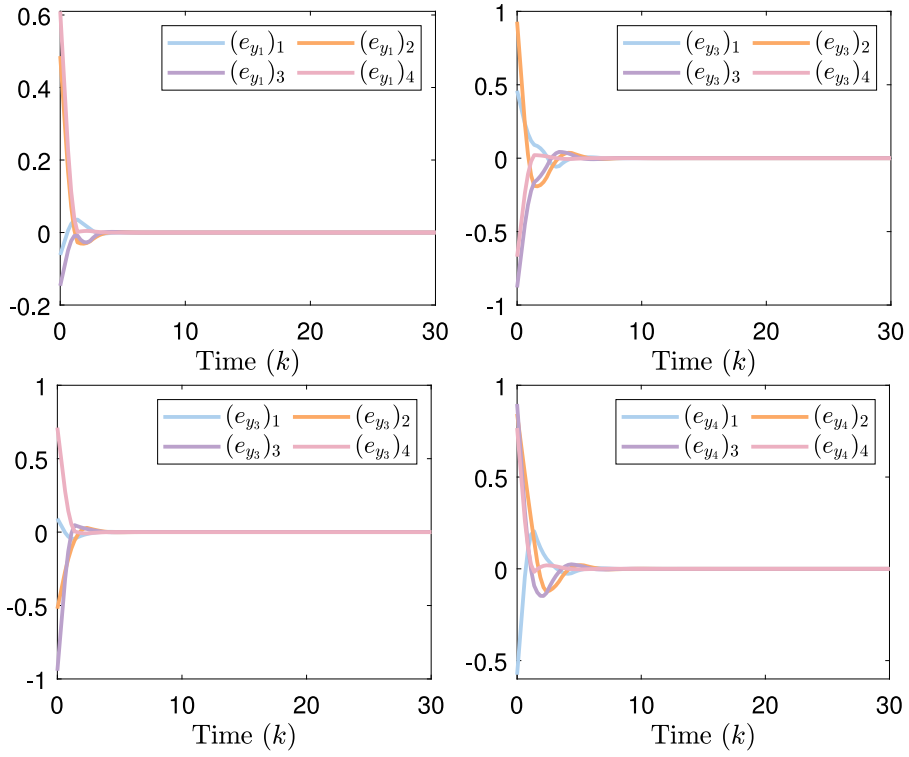

Fig. 2. Estimation errors of output under decentralized RMO in each agent.

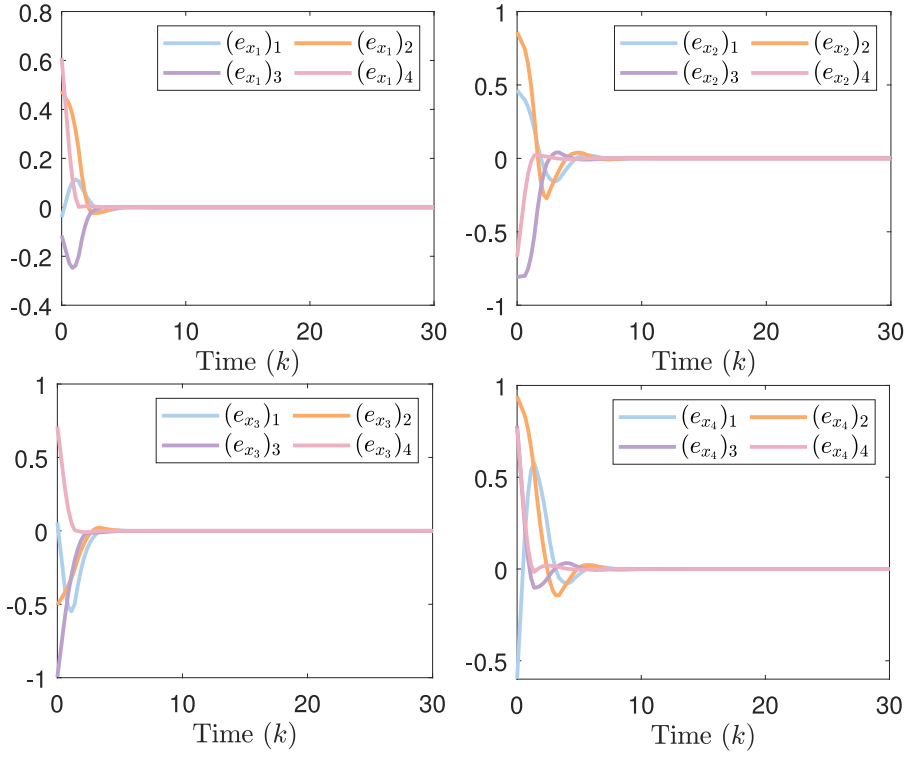

Fig. 3. Estimation errors of uncompromised state under decentralized RMO in each agent.

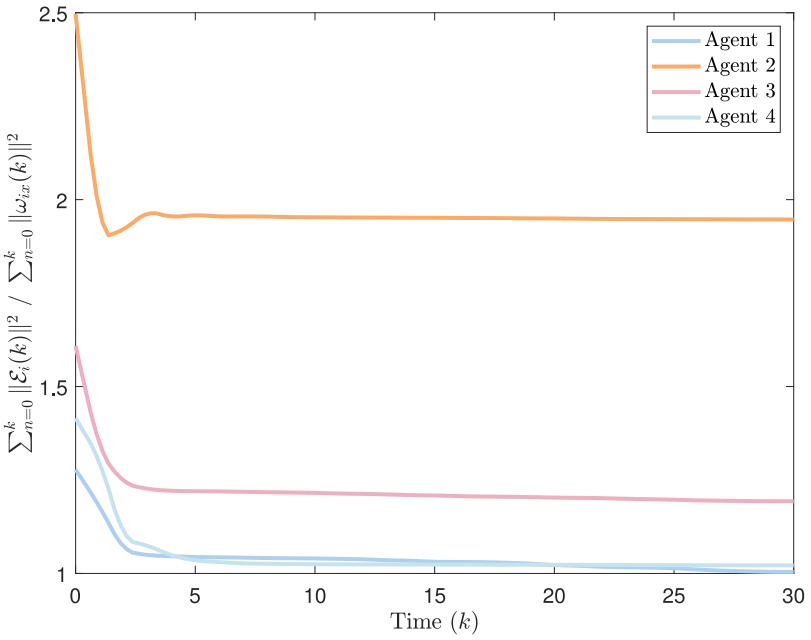

Fig. 4. H_∞ estimation performance of decentralized RMO in each agents.

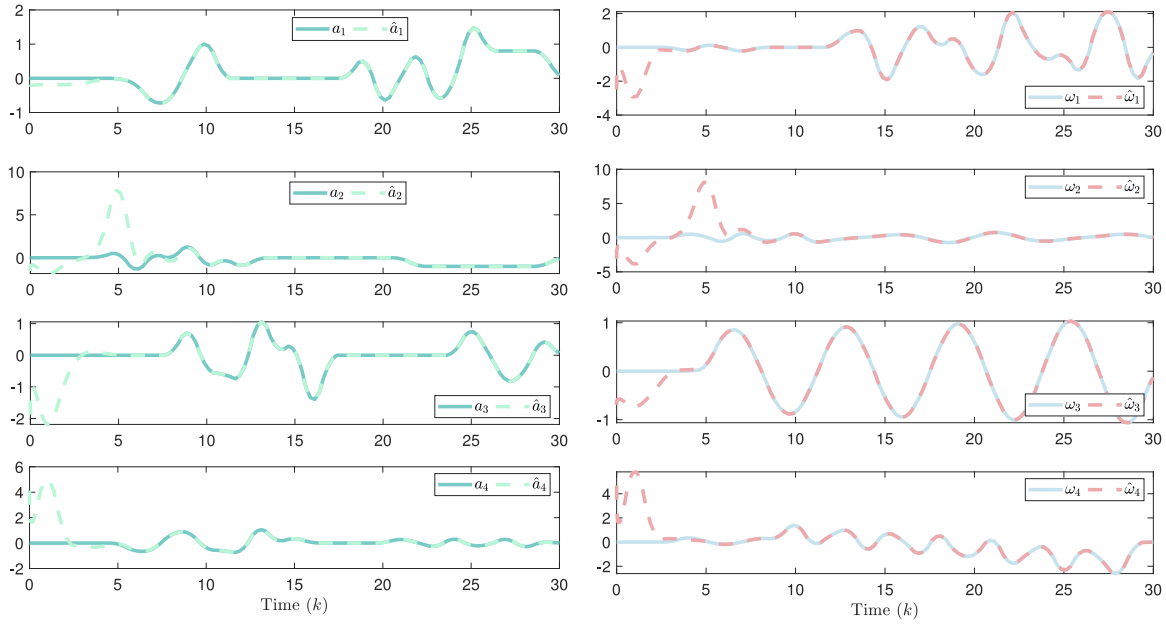

(a) FDI attacks (b) measurement disturbances

Fig. 5. Estimations of FDI attacks and measurement disturbances in each agent.

dynamic properties of the error Eq. (28). Through the fact that each agent has a minimum triggering interval of 2 and a maximum triggering interval that cannot exceed the projected time domain, the conclusion of Lemma 2 is verified, and the efficacy of the adjustable parameters is demonstrated. The Zeno phenomena can be successfully avoided by the trigger threshold proposed in this paper. The triggering interval in the control structure can set the distributed predictive controller to sleep, which can efficiently conserve computing resources.

From the simulation results, the proposed event-triggered DOFMPC scheme ensures the cooperation of the nonlinear MAS under S–C FDI attacks and disturbances. The uncompromised states, FDI attacks, and measurement disturbances are estimated and separated by the RMO simultaneously. The distributed output feedback model predictive controller handles the disturbances successfully and the event-triggered mechanism helps the controller to save a lot of computing resources. All the above verified the robust secure performance of our proposed framework.

6. Conclusion

This paper has proposed an event-triggered DOFMPC scheme to address the secure robust problem of nonlinear MAS with S–C FDI attacks and disturbances. The invalidity of compromised signals is overcome by a decentralized RMO, while the impacts of disturbances are eliminated by a newly-designed robustness constraint and an event-triggered mechanism. Theoretical analyses

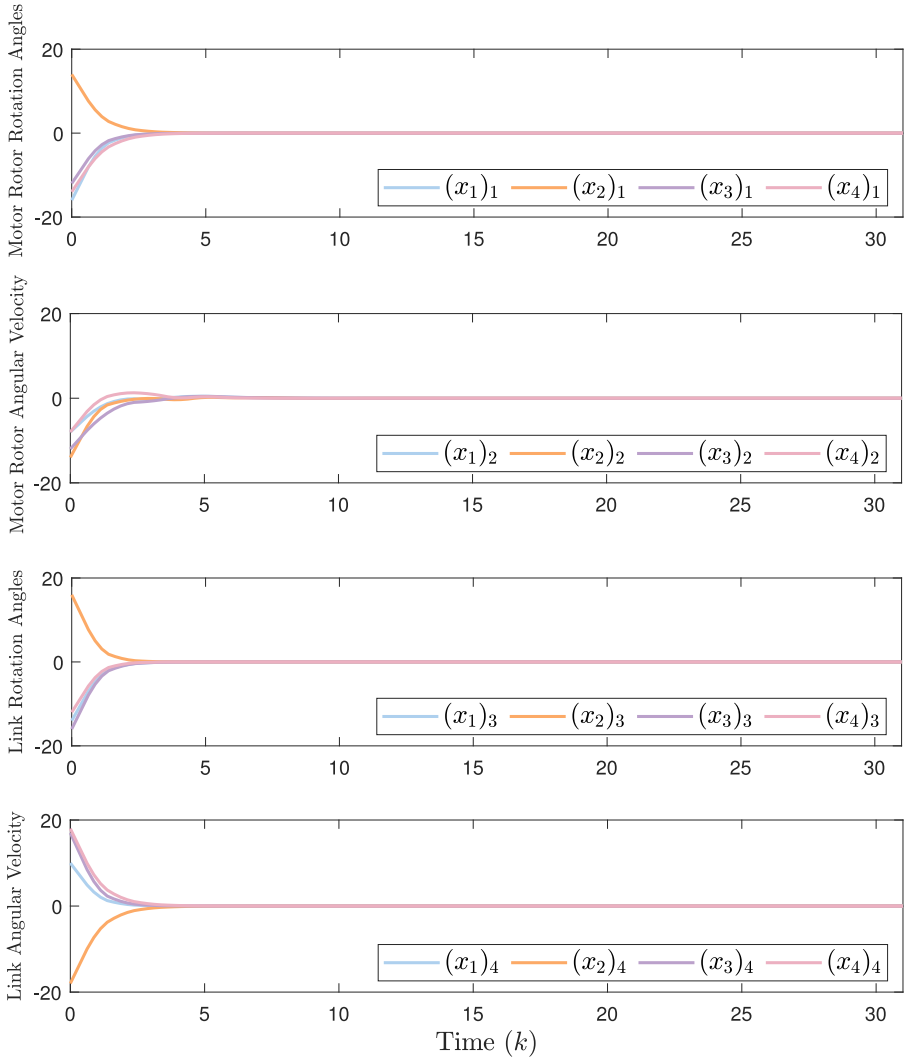

Fig. 6. Motor rotor rotation angles, motor rotor angular velocity, link rotation angles, and link angular velocity trajectories of each agent under event-triggered DOFMPC scheme.

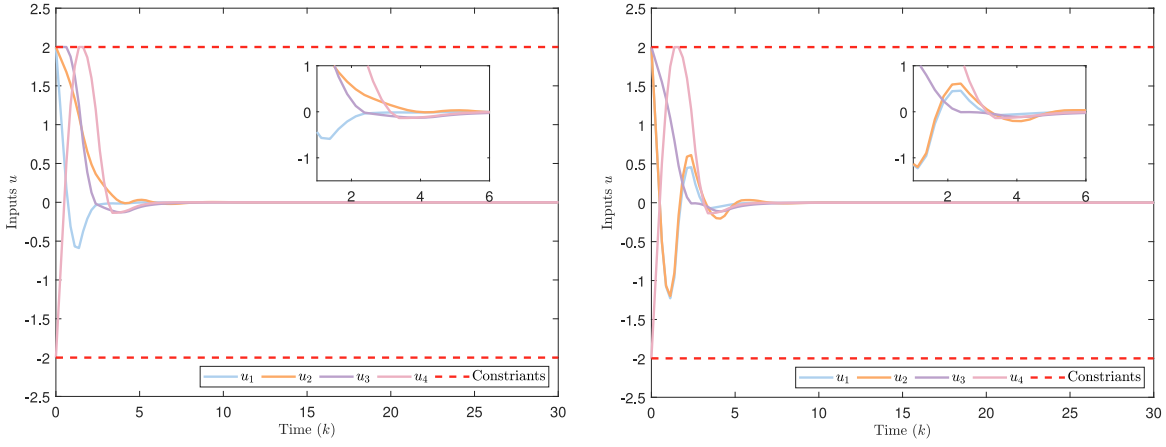

(a) event-triggered DOFMPC scheme with linear robustness constraints (b) robust DMPC scheme with inversely proportional robustness constraints[8, 9, 12]

Fig. 7. Control inputs of each agent under DMPC with different robustness constraints.

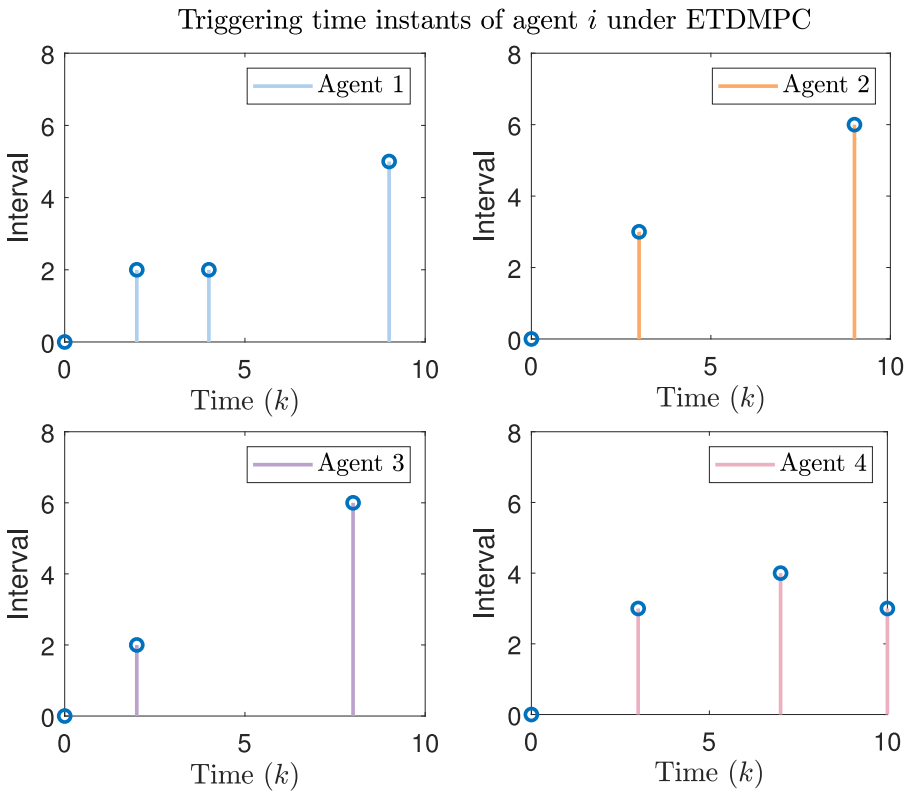

Fig. 8. Event Triggering time instants and intervals of each agent under event-triggered DOFMPC scheme.

on the recursive feasibility and cooperation of MAS are presented, and it is further demonstrated by simulation results. The current research shows that there is a large potential scope for using DOFMPC to provide secure control solutions for MAS.

Declaration of competing interest

No conflict of interest exits in the submission of this manuscript, and manuscript is approved by all authors for publication. I would like to declare on behalf of my co-authors that the work described was original research that has not been published previously, and not under consideration for publication elsewhere, in whole or in part. All the authors listed have approved the manuscript that is enclosed.

Acknowledgments

This work was supported in part by the National Natural Science Foundation of China [Grant number 61673218] and in part by the Postgraduate Research & Practice Innovation Program of Jiangsu Province [Grant numbers KYCX21_0246, KYCX21_0251].

References

[1] Olfati-Saber R, Fax JA, Murray RM. Consensus and cooperation in networked multi-agent systems. Proc IEEE 2007;95(1):215–33. http://dx.doi.org/10.1109/JPROC.2006.887293.

[2] Amirkhani A, Barshooi AH. Consensus in multi–agent systems: A review. Artif Intell Rev 2022;55:3897–935. http://dx.doi.org/10.1007/s10462-021-10097-x.

[3] Hu A, Park JH, Hu M. Consensus of nonlinear multiagent systems with intermittent dynamic event-triggered protocols. Nonlinear Dynam 2021;104:1299–313. http://dx.doi.org/10.1007/s11071-021-06321-6.

[4] Ren W, Beard RW, Atkins EM. Information consensus in multivehicle cooperative control. IEEE Control Syst Mag 2007;27(2):71–82. http://dx.doi.org/10.1109/MCS.2007.338264.

[5] Su H, Wang X, Lin Z. Flocking of multi-agents with a virtual leader. IEEE Trans Automat Control 2009;54(2):293–307. http://dx.doi.org/10.1109/TAC.2008.2010897.

[6] Ding D, Han Q-L, Wang Z, Ge X. A survey on model-based distributed control and filtering for industrial cyber-physical systems. IEEE Trans Ind Inf 2019;15(5):2483–99. http://dx.doi.org/10.1109/TII.2019.2905295.

[7] Yang Y, Xi X, Miao S, Wu J. Event-triggered output feedback containment control for a class of stochastic nonlinear multi-agent systems. Appl Math Comput 2022;418:126817. http://dx.doi.org/10.1016/j.amc.2021.126817.

[8] Li H, Shi Y. Robust distributed model predictive control of constrained continuous-time nonlinear systems: A robustness constraint approach. IEEE Trans Automat Control 2014;59(6):1673–8. http://dx.doi.org/10.1109/TAC.2013.2294618.

[9] Li H, Shi Y. Distributed receding horizon control of large-scale nonlinear systems: Handling communication delays and disturbances. Automatica 2014;50(4):1264–71. http://dx.doi.org/10.1016/j.automatica.2014.02.031.

[10] Zhang J, Zhang H, Cai Y, Wang W. Consensus control for nonlinear multi-agent systems with event-triggered communications. Appl Math Comput 2021;408:126341. http://dx.doi.org/10.1016/j.amc.2021.126341.

[11] Li Z, Ren W, Liu X, Fu M. Consensus of multi-agent systems with general linear and Lipschitz nonlinear dynamics using distributed adaptive protocols. IEEE Trans Automat Control 2013;58(7):1786–91. http://dx.doi.org/10.1109/TAC.2012.2235715.

[12] Zhou Y, Li D, Xi Y, Gao F. Event-triggered distributed robust model predictive control for a class of nonlinear interconnected systems. Automatica 2022;136:110039. http://dx.doi.org/10.1016/j.automatica.2021.110039.

[13] Zhang D, Wang Q-G, Feng G, Shi Y, A.V. Vasilakos. A survey on attack detection, estimation and control of industrial cyber–physical systems. ISA Trans 2021;116:1–16. http://dx.doi.org/10.1016/j.isatra.2021.01.036.

[14] Dong L, Xu H, Wei X, Hu X. Security correction control of stochastic cyber–physical systems subject to false data injection attacks with heterogeneous effects. ISA Trans 2022;123:1–13. http://dx.doi.org/10.1016/j.isatra.2021.05.015.

[15] Arauz T, Chanfreut P, Maestre JM. Cyber-security in networked and distributed model predictive control. Annu Rev Control 2022;53:338–55. http://dx.doi.org/10.1016/j.arcontrol.2021.10.005.

[16] Chen J, Zhang H, Yin G. Distributed dynamic event-triggered secure model predictive control of vehicle platoon against DoS attacks. IEEE Trans Veh Technol 2023;72(3):2863–77. http://dx.doi.org/10.1109/TVT.2022.3215966.

[17] Xue Y, Ren W, Zheng B-C, Han J. Event-triggered adaptive sliding mode control of cyber–physical systems under false data injection attack. Appl Math Comput 2022;433:127403. http://dx.doi.org/10.1016/j.amc.2022.127403.

[18] Sun Y-C, Yang G-H. Robust event-triggered model predictive control for cyber–physical systems under denial-of-service attacks. Internat J Robust Nonlinear Control 2019;29(14):4797–811. http://dx.doi.org/10.1002/rnc.4654.

[19] Li B, Zhou X, Ning Z, Guan X, Yiu K-FC. Dynamic event-triggered security control for networked control systems with cyber-attacks: A model predictive control approach. Inform Sci 2022;612:384–98. http://dx.doi.org/10.1016/j.ins.2022.08.093.

[20] Franze G, Famularo D, Lucia W, Tedesco F. A resilient control strategy for cyber–physical systems subject to denial of service attacks: A leader-follower set-theoretic approach. IEEE/CAA J Autom Sin 2020;7(5):1204–14. http://dx.doi.org/10.1109/JAS.2020.1003189.

[21] Yang H, Li Y, Dai L, Xia Y. MPC-based defense strategy for distributed networked control systems under DoS attacks. Syst Control Lett 2019;128:9–18. http://dx.doi.org/10.1016/j.sysconle.2019.04.001.

[22] Franzè G, Tedesco F, Famularo D. Resilience against replay attacks: A distributed model predictive control scheme for networked multi-agent systems. IEEE/CAA J Autom Sin 2021;8(3):628–40. http://dx.doi.org/10.1109/JAS.2020.1003542.

[23] Hu Z, Liu S, Luo W, Wu L. Intrusion-detector-dependent distributed economic model predictive control for load frequency regulation with PEVs under cyber attacks. IEEE Trans Circuits Syst I, Reg Pap 2021;68(9):3857–68. http://dx.doi.org/10.1109/TCSI.2021.3089770.

[24] Copp DA, Vamvoudakis KG, Hespanha JP. Distributed output-feedback model predictive control for multi-agent consensus. Syst Control Lett 2019;127:52–9. http://dx.doi.org/10.1016/j.sysconle.2019.04.005.

[25] Razavinasab Z, Farsangi MM, Barkhordari M. Robust output feedback distributed model predictive control of networked systems with communication delays in the presence of disturbance. ISA Trans 2018;80:12–21. http://dx.doi.org/10.1016/j.isatra.2018.07.003.

[26] Zhang S, Zhao D, Spurgeon SK. Distributed static output feedback robust model predictive control for process networks. Control Eng Pract 2022;126:105239. http://dx.doi.org/10.1016/j.conengprac.2022.105239.

[27] Souza AR, Efimov D, Raïssi T, Ping X. Robust output feedback model predictive control for constrained linear systems via interval observers. Automatica 2022;135:109951. http://dx.doi.org/10.1016/j.automatica.2021.109951.

[28] Ping X, Wang X, Lin T, Ding B, Polyakov A. An off-line approach for output feedback robust model predictive control. J Franklin Inst 2021;358(17):9263–87. http://dx.doi.org/10.1016/j.jfranklin.2021.09.006.

[29] Yang Y, Ding B, Xu Z, Zhao J. Tube-based output feedback model predictive control of polytopic uncertain system with bounded disturbances. J Franklin Inst 2019;356(15):7990–8011. http://dx.doi.org/10.1016/j.jfranklin.2019.06.010.

[30] Li J, Wang Q, Su Y, Sun C. Robust distributed model predictive consensus of discrete-time multi-agent systems: A self-triggered approach. Front Inform Technol Electron Eng 2021;22:1068–79. http://dx.doi.org/10.1631/FITEE.2000182.

[31] Li Z, Xu H, Lin Z, Chen X, Ma C. Robust self-triggered DMPC for linear discrete-time systems with local and global constraints. J Franklin Inst 2023;360(1):527–54. http://dx.doi.org/10.1016/j.jfranklin.2022.09.044.

[32] Li J, Zhang W, Zhang Z, Li X, Yang X. Predictive control based on event-triggering mechanism of cyber–physical systems under denial-of-service attacks. Inform Sci 2022;586:294–309. http://dx.doi.org/10.1016/j.ins.2021.11.082.

[33] Gu Y, Yu X, Guo K, Qiao J, Guo L. Detection, estimation, and compensation of false data injection attack for UAVs. Inform Sci 2021;546:723–41. http://dx.doi.org/10.1016/j.ins.2020.08.055.

[34] Huang H, Li D, Xi Y. Mixed H_2/H_∞ robust model predictive control with saturated inputs. Internat J Systems Sci 2014;45(12):2565–75. http://dx.doi.org/10.1080/00207721.2013.773471.

[35] Yang Y, Xu H, Yue D. Observer-based distributed secure consensus control of a class of linear multi-agent systems subject to random attacks. IEEE Trans Circuits Syst I, Reg Pap 2019;66(8):3089–99. http://dx.doi.org/10.1109/TCSI.2019.2904747.

[36] Khalkhali MB, Vahedian A, Yazdi HS. Multi-target state estimation using interactive Kalman filter for multi-vehicle tracking. IEEE Trans Intell Transp Syst 2020;21(3):1131–44. http://dx.doi.org/10.1109/TITS.2019.2902664.

[37] Shi Y, Yu B. Output feedback stabilization of networked control systems with random delays modeled by Markov chains. IEEE Trans Automat Control 2009;54(7):1668–74. http://dx.doi.org/10.1109/TAC.2009.2020638.

[38] Shi Y, Yu B. Robust mixed H_2/H_∞ control of networked control systems with random time delays in both forward and backward communication links. Automatica 2011;47(4):754–60. http://dx.doi.org/10.1016/j.automatica.2011.01.022.

[39] Mayne DQ, Raković SV, Findeisen R, Allgöwer F. Robust output feedback model predictive control of constrained linear systems. Automatica 2006;42(7):1217–22. http://dx.doi.org/10.1016/j.automatica.2006.03.005.

[40] Michalska H, Mayne DQ. Robust receding horizon control of constrained nonlinear systems. IEEE Trans Automat Control 1993;38(11):1623–33. http://dx.doi.org/10.1109/9.262032.

[41] Dunbar WB. Distributed receding horizon control of dynamically coupled nonlinear systems. IEEE Trans Automat Control 2007;52(7):1249–63. http://dx.doi.org/10.1109/TAC.2007.900828.

[42] Jiang B, Staroswiecki M, Cocquempot V. Fault accommodation for nonlinear dynamic systems. IEEE Trans Automat Control 2006;51(9):1578–83. http://dx.doi.org/10.1109/TAC.2006.878732.